# HEAT TRANSFER IN TURBULENT SHEAR FLOW

Thesis by

William Duncan Rannie

In Partial Fulfillment of the Requirements

for the Degree of

Doctor of Philosophy

California Institute of Technology

Pasadena, California

1951

## ACKNOWLEDGMENTS

The author wishes to express his appreciation of the valuable criticism and discussion with Professor Hsue-shen Tsien during the progress of this research. Sincere thanks are due to Miss Esther Gilbert for typing the manuscript.

## ABSTRACT

A new and relatively simple description is proposed for the velocity profile in turbulent flow close to a smooth wall. Heat transfer coefficients are calculated from the description and are shown to agree better with experiment than other theories. The analysis is extended to transport processes in liquids where the viscosity has a large variation close to the wall.

TABLE OF CONTENTS

## SUMMARY

Since no exact theory for turbulent shear flow exists at the present time, the analysis of heat transfer must be made in terms of empirical formulas and semi-empirical theories. The empirical formulas give no insight into the transport mechanism and are not reliable outside the range of the experiments upon which they are based. The semi-empirical theories are derived from similarity hypotheses supplemented by a few constants taken from experiment. These theories have been remarkably successful in many situations but fail in others, indicating that they do not give a description of turbulent transport that is universally valid. The purpose of this investigation is to improve the phenomenological theories by extending their range of validity and by reducing the number of empirical constants. Pipe flow alone will be considered because of its simplicity and the availability of experimental results.

The present status of heat transfer theories is reviewed in some detail in Section I. Reynolds postulated that energy and momentum are transported in the same way in turbulent shear flow and this analogy forms the basis of all subsequent work. Prandtl and Taylor extended the analysis to take into account the molecular transport close to a smooth wall. Later Kármán improved the theory by considering a layer, between the laminar region at the wall and the turbulent core, in which molecular and turbulent transports are of comparable magnitudes. Measured velocity profiles were used to establish the thicknesses of the layers and the momentum transport laws. With the latter and the

Reynolds analogy, the heat transfer rates were found.

The method of Kármán is very satisfactory provided that the rates of molecular transport of heat and momentum are not too different. For many liquids, however, these rates differ by a large factor and if the thickness of the region of approximately laminar flow is chosen from momentum considerations, the effectively laminar region for heat transfer may be grossly overestimated. Kármán's theory fails when the molecular transport of heat is much less than the equivalent transport of momentum and empirical formulas only have been available under these circumstances. Another restriction of the Kármán theory is that there is no way of introducing the effect of variable viscosity in the region close to the wall when the rate of heat transfer is high. Engineering applications of high rates of heat transfer to liquids with viscosity strongly dependent on temperature are becoming increasingly important.

A new law for the turbulent part of the shear stress in the wall region is proposed in Section II. The essential improvement over Kármán's method is that it is not necessary to assume a completely laminar layer next the wall; the turbulent shear stress is taken into account throughout the wall layer. A further advantage is that the thickness of the wall layer is determined from the two empirical constants describing the velocity profile in the turbulent core. The new law is not based on a similarity hypothesis, however, and hence its validity can be judged only by the consistency of results deduced from it and compared with experiment. The velocity profile derived from application of the law is satisfactory, although this comparison does not give a sharp criterion.

The new law is combined with the Reynolds analogy in Section III. to calculate heat transfer coefficients. These are compared with experiments and although there is considerable scatter in the latter, the law is confirmed within the error of measurement. It appears to be quite satisfactory in the range where Kármán's formula fails.

In Section IV. the turbulent shear stress law is applied to momentum transport where the viscosity varies in the region close to the wall. The turbulent fluctuations close to the wall are treated as forced oscillations and a simple model is assumed for calculating the effect of the viscosity change on the turbulent shear stress where most of the change takes place near the wall. The influence of density variation on the shear stress is not known so the theory is confined to liquids. Most non-metallic liquids have sufficiently large Prandtl numbers ($C_p\mu/k$) that the assumption that the viscosity variation is confined to the wall layer is not very restrictive.

In Section V., the addition of the Reynolds analogy to the theory of Section IV. allows calculation of the heat transfer coefficient for variable specific heat and conductivity as well as viscosity. Comparisons of calculated and measured friction and heat transfer coefficients are made in Section VI. The only tests that have been found suitable for this purpose were experiments on n-butyl alcohol made at the Jet Propulsion Laboratory. The friction coefficients are found to be in almost perfect agreement. The calculated heat transfer coefficients are found to be too high by 30% or so at ratios of bulk to wall viscosity greater than 5. Unfortunately, the conductivity variation with temperature is not known and it was assumed constant in the analysis.

The conductivity is known to decrease with temperature and this variation tends to bring the theory into line with experiment. Whether or not the conductivity variation is sufficient to explain all of the discrepency between theory and experiment is not clear at present.

The conclusions resulting from the investigation can be summarized as follows:

(a) A new law for the turbulent shear stress in the wall layer has been postulated and, assuming the Reynolds analogy to hold, is proved to be correct within the limits of experimental error in heat transfer and velocity profile measurements. In particular the theory is correct for large Prandtl numbers where the earlier Kármán theory is deficient.

(b) With some reasonable assumptions as to the influence of variable viscosity on the turbulent transport mechanism, the new theory has been applied to transfer processes at high rates of heat flux, in liquids. Variable specific heat and conductivity can be taken into account. This extended theory is correct, approximately at least, but cannot be proved or disproved completely until the variation of conductivity with temperature is better known.

(c) Few experiments of sufficient accuracy for determining the validity of the theory are available. In planning further accurate heat transfer measurements, it must be kept in mind that unless the variations of all physical properties are known, the experimental results will be of limited use for checking a theory.

# I. INTRODUCTION

The first important step in the analysis of heat transfer in turbulent flow was made by Reynolds, who postulated that energy and momentum are transferred in the same way in turbulent shear flow (Ref. 1, 1874). In order to demonstrate his theory, and subsequent refinements, consider the equations of momentum and energy, averaged with respect to time, for mean flow parallel to a wall. These are:

$$\tau = \tau_o = -\rho \overline{u'v'} + \mu \frac{du}{dy} \tag{1.1}$$

$$q = q_o = -\rho c_p \overline{T'v'} + k \frac{dT}{dy} \tag{1.2}$$

where $\tau_o$ is the shear stress at the wall and $q_o$ is the heat flow rate per unit area normal to the wall. A discussion of the derivation of these well known equations is given in Appendix A; for the time being it is sufficient to state the principal assumptions. These are (a) the density $\rho$, the viscosity $\mu$, the specific heat $c_p$ and the conductivity $k$ are constant, (b) the temperature gradient $\partial T/\partial x$, along the wall, is neglected in comparison with the gradient $\partial T/\partial y$ normal to the wall and (c) the shear stress and rate of heat flux are independent of distance from the wall. This last assumption will be approximately correct for pipe flow, provided that the distance from the wall is small compared with the pipe radius.

The Reynolds analogy, as the postulate is usually called, can be expressed quantitatively by the equation:

$$\frac{q_o}{\rho c_p dT/dy} = \frac{\tau_o}{\rho\, du/dy} \tag{1.3}$$

which states, in effect, that the rate of energy transport normal to the wall bears the same relation to the energy gradient as the shear stress bears to the momentum gradient. Integrating (1.3) between the wall, where $u$ is zero and some station where $u$ and $T$ can be considered as attaining mean values, as denoted by the subscript $m$ :

$$\frac{q_0}{\rho c_p (T_m - T_w) u_m} = \frac{\tau_0}{\rho u_m^2} \tag{1.4}$$

or

$$C_h = \tfrac{1}{2} C_f \tag{1.5}$$

where $C_h$ and $C_f$ are the heat transfer and friction coefficients, respectively.

The theory as given above ignores the molecular transport terms in Eqs. (1.1) and (1.2). If these equations are rearranged in the forms:

$$\tau_0 = \rho \left( - \frac{\overline{u'v'}}{du/dy} + \nu \right) \frac{du}{dy} \tag{1.6}$$

$$q_0 = \rho c_p \left( - \frac{\overline{T'v'}}{dT/dy} + \nu/\sigma \right) \frac{dT}{dy} \tag{1.7}$$

where $\sigma = c_p \mu / k$ is the Prandtl number and $\nu = \mu/\rho$ is the kinematic viscosity, it can be seen that if the Reynolds analogy applies to the turbulent transport terms, and if $\sigma = 1$, Eq. (1.5) applies even when the flow is partially laminar. However, if $\sigma \neq 1$, the Reynolds analogy cannot hold for a laminar region, next a smooth wall, for instance.

The first extensions of the theory of Reynolds to fluids with Prandtl numbers differing from unity were made by Taylor (Ref. 2, 1919) and Prandtl (e.g. Ref. 3, 1928). Their refinements were similar and the latter only will be indicated here. Prandtl assumed a layer of

purely laminar flow between the wall and a completely turbulent core. Denoting by $y_1$ the distance of the outer edge of the laminar layer, Prandtl obtained:

$$\left.\begin{aligned} \frac{\tau_0}{\rho} &= \nu \frac{du}{dy} = \nu \frac{u_1}{y_1} \qquad (1.8)\\ \frac{q_0}{\rho c_p} &= k \frac{dT}{dy} = \frac{\nu}{\sigma} \frac{T_1 - T_w}{y_1} \qquad (1.9) \end{aligned}\right\} \quad 0 < y < y_1$$

$$\frac{\tau_0}{\rho(u_m - u_1)} = \frac{q_0}{\rho c_p (T_m - T_1)} \qquad y > y_1 \qquad (1.10)$$

the last equation arising from the application of the Reynolds analogy from the edge of the core to the "mean" distance. Eliminating $T_1$ and $u_1$ from these three equations, he found:

$$\frac{1}{C_h} = \frac{2}{C_f}\left[1 + (\sigma - 1)\frac{y_1}{\nu u_m}\frac{\tau_0}{\rho}\right]$$

Defining a "friction velocity" $u_\tau = \sqrt{\tau_0/\rho}$ , this equation becomes:

$$\frac{1}{C_h} = \frac{2}{C_f} + (\sigma - 1)\frac{y_1 u_\tau}{\nu}\sqrt{\frac{2}{C_f}} \qquad (1.11)$$

From empirical expressions for the friction coefficient for pipes Prandtl deduced that $y_1 u_\tau/\nu = 5.6$ gave the best dimensionless thickness for the laminar layer.

The relation (1.11) between the heat transfer and friction coefficients is satisfactory for $\sigma$ quite close to unity but cannot be expected to hold for large or small values of $\sigma$. Kármán (Ref. 4, 1934 and Ref. 5, 1939) improved Prandtl's theory by assuming three distinct layers, a purely laminar sub-layer next the wall, a buffer layer in which turbulent and molecular transport processes are of comparable importance, and a completely turbulent core. In the laminar sub-layer Kármán assumed Eq. (1.8) to hold and in the core the logarithmic law:

$$u/u_\tau = 2.5 \ln y^* + 5.5 \qquad y^* \gtrsim 30 \qquad (1.12)$$

where $y^* = y u_\tau/\nu$ is the dimensionless distance from the wall. The form of this equation had been derived previously by similarity hypotheses and the constants were determined from experiments (e.g. Ref. 6, p. 333). For the buffer layer, Kármán assumed a velocity profile of the same form as (1.12), that is:

$$u/u_\tau = a \ln y^* + b \qquad (1.13)$$

where a and b are arbitrary constants.

Upon examination of velocity profile measurements made by Nikuradze very close to a smooth wall, Kármán decided that the laminar profile (1.8) held out to $y^* = y_1^* = 5$ and the turbulent profile (1.12) held down to $y^* = y_2^* = 30$. Because of experimental difficulties (the distance $y_1^*$ corresponded to a few thousandths of an inch) the measurements may not have been very reliable and, in addition, there are no sharp dividing lines between layers. Kármán determined the two constants a and b in (1.13) so that u and du/dy were continuous at the edge of laminar sub-layer and so u was continuous at the edge of the core, hence:

$$a = y_1^* = 5 \qquad b = -y_1^*(\ln y_1^* - 1) = -3.05 \qquad (1.14)$$

Kármán, unlike other people, has no difficulty in finding two arbitrary constants to satisfy three conditions.

For the calculation of heat transfer, Kármán assumed that the Reynolds analogy held for turbulent transport in the buffer layer and

hence obtained, by substitution from Eq. (1.6) into Eq. (1.7):

$$\frac{q_o}{\rho C_p} = \left(-\frac{\overline{u'v'}}{du/dy} + \nu/\sigma\right)\frac{dT}{dy} = \left[\frac{u_\tau^2}{du/dy} - \nu\left(1-\frac{1}{\sigma}\right)\right] \qquad (1.15)$$

Since $du/dy = a u_\tau/y$ in the buffer layer, Eq. (1.15) can be integrated between $y_1^*$ and $y_2^*$ to give:

$$\frac{\rho C_p u_\tau}{q_o}(T_2-T_1) = a \ln \frac{y_2^*/a - 1 + 1/\sigma}{y_1^*/a - 1 + 1/\sigma} \qquad (1.16)$$

Expressions for $T_1-T_w$ and $T_m-T_2$ can be found from Eqs. (1.9) and (1.10) (with $u_2$ and $T_2$ for $u_1$ and $T_1$ in the latter); by addition to Eq. 1.15, substitution for a and b from (1.14) and a little manipulation, one obtains:

$$\frac{1}{C_h} = \frac{2}{C_f} + y_1^*\left[(\sigma-1) + \ln\left\{1+(\sigma-1)(1-y_1^*/y_2^*)\right\}\right]\sqrt{\frac{2}{C_f}} \qquad (1.17)$$

and substituting $y_1^* = 5$, $y_2^* = 30$:

$$\frac{1}{C_h} = \frac{2}{C_f} + 5\left[(\sigma-1) + \ln\left\{1+0.83(\sigma-1)\right\}\right]\sqrt{\frac{2}{C_f}} \qquad (1.18)$$

For $\sigma$ approaching unity the coefficient of $\sqrt{2/C_f}$ is $9.2(\sigma-1)$ as compared with $5.6(\sigma-1)$ obtained by Prandtl.

The effect of varying the Prandtl number is to change the relative proportions of molecular to turbulent transport at any given distance from the wall. This can be seen by comparing the two terms in parentheses in Eq. (1.15); the first term, corresponding to turbulent transport and resulting from the Reynolds analogy, involves velocities only and remains constant for fixed y, while the second term $\nu/\sigma$ changes withthe Prandtl number. Increasing $\sigma$ causes the turbulent transport term to become relatively more important in the region close

to the wall. Kármán's reason for introducing the buffer layer was to include a region in which both types of transport mechanism were represented, so their relative magnitudes could be varied with changes in Prandtl number. His theory agrees well with experiments on water, with a Prandtl number of 10 or so, but at very high values of $\sigma$, 50 to 100 say, the deviation from measurements is very large. For $\sigma$ large, the term $2/C_f$ becomes negligible in comparison with the other term on the right hand side of Eq. (1.18). Kármán's equation predicts $C_h$ proportional to $1/\sigma$ for $\sigma$ very large; it is well known from measurements that $C_h$ is more nearly proportional to $1/\sqrt{\sigma}$ under these circumstances.

The reason for the failure of Kármán's theory at large Prandtl numbers is not difficult to find. The outer edge of the laminar layer was identified with the point at which the measured velocity profile first appeared to deviate from a laminar profile. There is no precise point of deviation and besides there was scatter in the measurements. At $y^* = 5$ a small portion of the momentum transport undoubtedly results from turbulence. For the sake of argument, let us say that 5% of the shear stress at $y^* = 5$ is turbulent; certainly this is the minimum amount that could be detected from examination of the velocity profile. This is negligible as far as momentum transfer is concerned, but it can be magnified into an appreciable fraction of the total energy transport if the Prandtl number is large. For instance, at $\sigma = 10$ the turbulent transport of energy would become 33% of the total, and in Kármán's theory this would be neglected. The relative amount of turbulent transfer will decrease rapidly toward the wall so the net effect

of neglecting it will not be serious at Prandtl numbers of 10 or so. The situation is entirely different at very large values of $\sigma$; at $\sigma = 100$, for instance, 83% of the total energy transport would arise from turbulence and its neglect would increase the resistance of the sub-layer to heat flow by an appreciable fraction.

Shortly after Kármán's analysis appeared, Reichardt published a paper on turbulent heat transfer (Ref. 7, 1940). He also divided the flow into three regions but criticized Nikuradze's measurements, which Kármán had used as a basis for choice of the sub-layer thickness. Reichardt made his own measurements of the velocity profile and found some deviation from those of Nikuradze. He recognized the difficulty of allowing for the magnification of the turbulent momentum transport into energy transport at large Prandtl numbers and based his choice of $y_1^*$ on results of heat transfer measurements as well as the velocity profile. He found $y_1^* = 2$ to give the best agreement with experiment. Reichardt's representation of the buffer layer profile was somewhat more complicated than Kármán's and his final results are not as convenient for application. He did not believe that the Reynolds analogy held precisely and he introduced a "turbulent Prandtl number" bearing the same relation to the turbulent momentum and energy transports as $\sigma$ does to the molecular momentum and energy transports. He found that a turbulent Prandtl number of about 0.9 gave the best agreement of his theory with a limited number of experiments.

One of the most important problems in heat transfer at the present time concerns the influence of variable physical properties, particularly the viscosity. At very high rates of heat transfer in liquids the

viscosity may vary by a factor of five or more through the wall layers. The conductivities of liquids are not usually as sensitive functions of temperature as the viscosities and the effect of the variation of the former may not be so important. Kármán chose the thicknesses of the laminar sub-layer and the buffer layer from measurements in isothermal flow and because no measurements have been made with the viscosity varying, there is no direct experimental evidence of its influence on the profile. Reichardt, in the paper mentioned above, assumed that the velocity at the edge of the laminar sub-layer is constant, if the viscosity variation is confined to this layer, but that the laminar sub-layer thickness changes. No data to support this assumption were presented.

Boelter, Martinelli and Jonassen (Ref. 8, 1941) treated the influence of variable viscosity empirically. Starting from Kármán's equation in the form (1.17) they determined $y_1^*$ to give the best fit with measurements of heat transfer where the viscosity varied. They assumed a linear temperature gradient in the laminar sub-layer, and knowing the variation of viscosity with temperature, found the ratio of viscosity at the wall to the viscosity at $y_1^*$ . The viscosity was assumed constant and equal to the mean core value for $y^* > y_1^*$ . The final results consist of a table of $y_1^*$ as a function of viscosity ratio and Reynolds number which is to be used in conjunction with an equation essentially the same as (1.17). The authors claim better correlation of results from their semi-empirical theory than from the Kármán relation for other heat transfer measurements. The weakness of their method is that the variable $y_1^*$ may have no physical significance whatever.

The Prandtl numbers of fluids cover a very wide range, those of non-metallic liquids extending from 5 or so to as high as 1,000, while for metallic liquids $\sigma$ is very low, 0.01 or less. Gases have values of $\sigma$ from 0.65 to 0.8 but there is a large gap between the gases and metallic liquids in which no fluids appear to fall. For very low Prandtl numbers, Kármán's theory is not applicable; in fact, it was not intended for such conditions. Martinelli (Ref. 9, 1947) modified the theory to take into account molecular transport of energy throughout the flow. Because the conductivity is high, the mean temperature may occur at a distance from the wall that is an appreciable fraction of the pipe radius (unless the Reynolds number is extremely large) and hence $q_0$ in Eq. (1.2) is replaced by $q_0(1 - y/R)$ where R is the pipe radius. Actually, this is the more correct form for q, just as $\tau = \tau_0(1-y/R)$ is strictly correct for the shear stress. In the turbulent core Martinelli used Eq. (1.15) with this modification to $q_0$. The method of joining the solutions for the three layers is the same as used by Kármán, with the added complication of another parameter R. The heat transfer measurements at very low Prandtl numbers are meager and probably unreliable, so it is scarcely possible to say whether the theory is satisfactory in this range.

Although many other papers on turbulent heat transfer in pipes have appeared, most have been concerned with empirical representation of measurements; those mentioned above seem to the writer to be the most significant contributions to the theory. Kármán's equation has remained, after eleven years, the most useful and reliable and most refinements to the theory start with it as a basis. Its deficiencies are appreciable only at very low and at very high Prandtl numbers and

at high rates of heat transfer where the values of the physical properties vary. Problems connected with these extreme conditions are, however, becoming increasingly important, as for instance the heat transfer in nuclear reactors to molten metals with very low Prandtl numbers, and the high heat fluxes in cooling of rocket motors. The requirements for a theory to improve on Kármán's are clear; these are (a) elimination of the completely laminar sub-layer so that, at very high Prandtl numbers, the important contribution of the turbulent transport of energy within this region is properly evaluated and (b) a method for determining the influence of variable viscosity on the turbulent transport processes near the wall. Knowledge of the underlying mechanism of turbulent transport in shear flow is very limited and hence the theory of heat transfer must of necessity be phenomenological in nature. The evils of the empirical constants that invariably accompany such a theory make a third requirement essential if it is to be useful; it must be simple. The key to the analysis of heat transfer is an adequate description of the velocity profile at the wall. It is with this description that the section following is concerned.

## II. MOMENTUM TRANSFER IN ISOTHERMAL FLOW

The momentum equation, averaged with respect to time, for turbulent flow in a pipe is:

$$\tau_o (1 - y/R) = -\rho \overline{u'v'} + \mu \frac{du}{dy} \qquad (2.1)$$

where $y$ is the distance from the wall, $R$ is the pipe radius and is the shear stress at the wall. This equation is exact for fully developed turbulent flow if the physical properties are constant. A more complete discussion of the derivation of this equation is given in Appendix A. The analysis in this section will be concerned with distances $y$ that are much less than $R$, so that $y/R$ can be neglected in the first term. The turbulent shear stress $-\rho\overline{u'v'}$ must be zero at the wall since the velocity is zero there, but will increase with $y$ so that far enough from the wall it dominates the viscous shear stress completely.

Exact knowledge of the mechanism of turbulent exchange does not exist, hence the evaluation of $\overline{u'v'}$ in (2.1) and its dependence on physical and geometrical parameters must be deduced from measurements. Outside of the region where the laminar shear stress is important, similarity arguments have been applied with considerable success. For instance, one might assume that $\overline{u'v'}$ depends on distance $y$ from the wall, since there is less "restriction" further from the wall, and also on the velocity gradient $du/dy$, because this ratio is related to the difference of momentum between neighboring flow layers. Further, $\overline{u'v'}$ might depend on derivatiyes of the velocity of higher order, but probably not on the velocity $u$ directly.

The simplest combination of the relevant parameters that is dimensionally correct leads to the assumption:

$$\overline{u'v'} = -K\, y^2 \left(\frac{du}{dy}\right)^2 = -\tau_o/\rho \qquad (2.2)$$

where $K$ is a constant. Integrating this equation one obtains:

$$u^* = \frac{1}{\sqrt{K}} \ln y^* + B \qquad (2.3)$$

with the notation:

$$u_\tau = \sqrt{\tau_o/\rho} \qquad u^* = u/u_\tau \qquad y^* = y u_\tau/\nu \qquad (2.4)$$

and where $B$ is a constant. The expression (2.3) is the familiar logarithmic formula given by Kármán (Ref. 10, 1930) and extensive measurements in pipes (Ref. 6, p. 333) have demonstrated that it represents the velocity profile quite well for $y^* > 30$ if the Reynolds number $2Ru_m/\nu$ is greater than about 10,000. The values of the constants that fit the experiments best are:

$$\frac{1}{\sqrt{K}} = 2.5 \qquad B = 5.5 \qquad (2.5)$$

With these constants in Eq. (2.3) the profile fits well even to the center of the pipe, although it cannot be strictly correct there. The expression (2.2) chosen for $\overline{u'v'}$ is not unique; other formulations of the similarity hypothesis, depending on higher order derivatives, lead to a logarithmic relation for the velocity profile.

The velocity profile (2.3) is not satisfactory for $y^* < 30$ and the reason for this is certainly connected with the neglect of the viscous shear term near the wall. If this term is added, one obtains,

instead of (2.2):

$$\tau_o/\rho = K y^2 \left(\frac{du}{dy}\right)^2 + \nu \frac{du}{dy} \tag{2.6}$$

This equation can be integrated giving:

$$u^* = \frac{1}{\sqrt{K}} \sinh^{-1}\left(2\sqrt{K}\, y^*\right) - \frac{1}{2K y^*}\left(\sqrt{1+4K y^{*2}} - 1\right) \tag{2.7}$$

A comparison of this profile with measurements close to the wall shows, however, a large deviation in the wall region. The conclusion is that the similarity law for the shear stress in the completely turbulent region does not hold in the region where viscous shear stress is appreciable.

In searching for a law to represent the turbulent shear stress in the region of partially laminar flow, the author believed that the shear stress should be related to the local mean velocity rather than to distance from the wall or velocity gradient, as in the turbulent core. If this is correct, the simplest form for the turbulent shear stress is:

$$-\rho \overline{u'v'} = \rho K_1 u^2 \tag{2.8}$$

where $K_1$ is a constant. The method employed in obtaining this relation is analogous to that used for the fully turbulent region, although it is unlikely that a true similarity law holds in the wall region. Whether or not (2.8) has a real physical meaning is not known. If it can be proved that it gives a good description of the variation of turbulent shear stress, it will serve its purpose. The only precaution that need be observed is to avoid using it in situations where it takes

on physical significance. Experiment alone can show whether or not (2.8) represents conditions near the wall, just as experiment was required to justify the logarithmic law in the turbulent core.

The momentum equation becomes, after introducing (2.8):

$$\tau_0/\rho = u_\tau^2 = K_1 u^2 + \nu \frac{du}{dy} \tag{2.9}$$

The solution of this equation, satisfying the boundary condition $u = 0$ at $y = 0$, is in dimensionless form:

$$u^* = \frac{1}{\sqrt{K_1}} \tanh\left(\sqrt{K_1}\, y^*\right) \tag{2.10}$$

The laminar shear stress near the edge of the turbulent core is quite small and its effect can be taken into account by solving (2.6) for $du/dy$ and expanding in a series. Retaining the first two terms only:

$$\frac{du^*}{dy^*} = \frac{1}{\sqrt{K}} \frac{1}{y^*} - \frac{1}{2K y^{*2}} + \cdots \tag{2.11}$$

and integrating:

$$u^* = \frac{1}{\sqrt{K}} \ln y^* + B + \frac{1}{2K y^*} + \cdots \tag{2.12}$$

For large $y^*$ this reduces to the form (2.3). The contribution of the additional term is rather insignificant; it is included only to treat the momentum equation in a fashion parallel to the energy equation, where the conductivity term will be retained in the core.

The wall layer profile (2.10) must now be joined to the core profile (2.12). The values of $K$ and $B$ are known while $K_1$ must be determined. In order to have as smooth a junction as possible, $u^*$ and $du^*/dy^*$ will be made continuous and a second unknown, the junction

distance $y_1^*$ , introduced. The velocity gradient for the wall layer is, from (2.10):

$$\frac{du^*}{dy^*} = \operatorname{sech}^2(\sqrt{K_1}\, y^*) \qquad 0 < y^* < y_1^* \tag{2.13}$$

Equating velocities from (2.10) and (2.12) and gradients from (2.11) and (2.13) with $y^* = y_1^*$ , two equations for $K_1$ and $y_1^*$ are obtained:

$$\frac{1}{\sqrt{K_1}} \tanh(\sqrt{K_1}\, y_1^*) = 2.5 \ln y_1^* + 5.5 + \frac{3.125}{y^*} \tag{2.14}$$

$$\operatorname{sech}^2(\sqrt{K_1}\, y_1^*) = \frac{2.5}{y_1^*} - \frac{3.125}{y_1^{*2}} \tag{2.15}$$

and numerical solution of these gives:

$$y_1^* = 27.5 \qquad \frac{1}{\sqrt{K_1}} = 14.53 \tag{2.16}$$

If the laminar shear stress at the inner part of the turbulent core is neglected, the thickness of the wall layer is $y_1^* = 26.5$ , very close to the value above.

The velocity profile deduced above is compared with measured profiles and with Kármán's approximation in Fig. 1. The individual measured points are not indicated but it should be remembered that there is considerable scatter in the results of each of the investigators. The measurements are very difficult because the wall layer is quite thin under normal circumstances and the wall may influence instrument readings. None of the measurements can be considered really satisfactory. Laufer found a core profile in a two-dimensional channel quite different from pipe profiles. The conclusion from the comparison is that the theoretical profile deduced above is not less reliable than existing measure-

ments. The fact that $y_1^*$ turns out to be 27.5, quite close to the value 30 previously accepted from measurements, is perhaps the strongest argument that the turbulent shear stress in the wall layer is represented reasonably well by the assumed law.

It is interesting to see what the law above implies for the turbulent shear stress in the reginn previously called the laminar sub-layer. At $y^* = 5$, the edge of the sub-layer in Kármán's analysis, the turbulent shear stress is 12% of the total shear according to the new law and at $y^* = 2$, Reichardt's choice of the sub-layer thickness, 2% of the total shear stress. At the outer edge of the wall layer, corresponding approximately to the outer edge of the buffer layer, the turbulent shear stress is 91% of the total. The approximation of $\tau_0(1-y/R)$ by $\tau_0$ is not satisfactory at small Reynolds numbers. For instance, at a pipe Reynolds number of 5,000, $y_1/R = 0.18$ and at 10,000, $y_1/R = 0.09$; these terms are neglected in comparison with unity and hence the profile for the walllayer may not be satisfactory for Reynolds numbers less than 10,000 or so.

To sum up results: a promising analytical representation of the turbulent shear stress and the velocity profile has been found, a representation that is simple and eliminates the artificial laminar sub-layer previously assumed. It is not possible to determine the validity of the representation with any degree of accuracy from existing velocity profile measurements. The turbulent transport given by the proposed law will be used for calculation of heat transfer coefficients in the section following; the comparison with heat transfer

measurements over a wide range of Prandtl numbers will be a much more sensitive test of its accuracy.

## III. ENERGY TRANSFER WITH INVARIABLE PHYSICAL PROPERTIES

The energy equation, averaged with respect to time, for turbulent flow in a pipe at distances from the wall small compared with the pipe radius is:

$$q_o = -\rho C_p \overline{T'v'} + k \frac{dT}{dy} \tag{3.1}$$

where $q_o$ is the rate of heat transfer normal to the wall (in the negative $y$ direction) and $C_p$ is the specific heat. It is assumed that the density $\rho$, the specific heat $C_p$ and the conductivity $k$ are constants and that the temperature gradient along the wall can be neglected in comparison with $dT/dy$. A more complete discussion of this equation is given in Appendix A.

In the analysis that follows, the Reynolds analogy will be assumed to hold so that, for the turbulent transport terms:

$$\frac{\overline{T'v'}}{dT/dy} = \frac{\overline{u'v'}}{du/dy} \tag{3.2}$$

The validity of this postulate has not been proved conclusively by experiment. Some investigators have suggested introducing a "turbulent Prandtl number" $\sigma_t$ so:

$$\frac{\overline{T'v'}}{dT/dy} = \frac{1}{\sigma_t} \frac{\overline{u'v'}}{du/dy}$$

Reichardt (Ref. 7) found various values of $\sigma_t$ for different types of flow but recommended $\sigma_t = 0.9$ for heat transfer calculations; Corrsin (Ref. 12) found $\sigma_t = 0.75$ in heated wakes and Sage (Ref. 13) found $\sigma_t = 0.83$ in a two-dimensional channel. As will be discussed later,

heat transfer measurements in pipes appear to correlate best with $\sigma_t = 1$. Possibly the Reynolds analogy holds well in the high shear regions close to the wall but does not hold in low shear regions. The direct measurements mentioned above were made far from a wall and hence may not be applicable to the turbulent transport close to the wall. In the absence of better information $\sigma_t$ will be put equal to unity in the remaining analysis. If it is found, at some future time, that another value of is more appropriate, this can be introduced without complication, provided that its value can be taken as constant.

Substituting (3.2) into (3.1) and re-arranging:

$$\frac{dT}{dy} = \frac{q_o}{-\rho c_p \frac{\overline{u'v'}}{du/dy} + k}$$

or in dimensionless form, introducing the Prandtl number $\sigma = c_p \mu / k$:

$$\frac{\rho c_p u_\tau}{q_o} \frac{dT}{dy^*} = \frac{1}{-\frac{\overline{u'v'}/u_\tau^2}{du^*/dy^*} + \frac{1}{\sigma}} \qquad (3.3)$$

Expressions for $\overline{u'v'}$ and $du^*/dy^*$ for both wall layer and core were found in the preceding section. Substituting from (2.2), (2.8), (2.10), (2.11) and (2.13) into (3.3), we find for the wall layer and the core, respectively:

$$\frac{\rho c_p u_\tau}{q_o} \frac{dT}{dy^*} = \frac{1}{\sinh^2(\sqrt{K_1}\, y^*) + \frac{1}{\sigma}} \qquad 0 < y^* < y_1^* \qquad (3.4)$$

$$\frac{\rho c_p u_\tau}{q_o} \frac{dT}{dy^*} = \frac{1}{\sqrt{K}\, y^* - \frac{1}{2} + \frac{1}{\sigma}} \qquad y^* > y_1^* \qquad (3.5)$$

Since $\overline{u'v'}$ and $du^*/dy^*$ are both continuous at $y^* = y1^*$, it can be seen from Eq. (3.3) that $dT/dy^*$ is continuous there as well.

The integration of Eqs. (3.4) and (3.5) can be done exactly and the resulting temperature distribution, in terms of the wall temperature $T_w$ and the temperature at the edge of the wall layer $T_1$, is:

$$\frac{\rho c_p u_\tau}{q_0}(T-T_w) = \frac{\sigma}{\sqrt{K_1}\sqrt{1-\sigma}} \tanh^{-1}\left(\sqrt{1-\sigma}\tanh\sqrt{K_1}y^*\right) \qquad \sigma<1 \qquad (3.6)$$

$$= \frac{\sigma}{\sqrt{K_1}\sqrt{\sigma-1}} \tan^{-1}\left(\sqrt{\sigma-1}\tanh\sqrt{K_1}y^*\right) \qquad \sigma>1 \qquad (3.7)$$

$$0<y^*<y_1^*$$

$$\frac{\rho c_p u_\tau}{q_0}(T-T_1) = \frac{1}{\sqrt{K}} \ln \frac{y^* + \frac{2-\sigma}{2\sqrt{K}\sigma}}{y_1^* + \frac{2-\sigma}{2\sqrt{K}\sigma}} \qquad y^*>y_1^* \qquad (3.8)$$

The temperature $T_1$ can be obtained from (3.6) or (3.7) by putting $y^* = y1^*$ .

The heat transfer coefficient is usually given in terms of the temperature difference $(T_m - T_w)$ where $T_m$ is a mean temperature of the fluid in the pipe. There are various ways of defining $T_m$ and it may be well to discuss these briefly. The simplest procedure is the one used by Prandtl, Kármán and others; they assumed that the distance from the wall at which the fluid temperature reaches the mean temperature is the same as the distance at which the velocity reaches the mean velocity. This is strictly correct only if the Prandtl number is unity, because then the temperature and velocity profiles are identical. At other values of $\sigma$ it will not be quite correct, the approximation becoming poorer as the Reynolds number decreases.

To apply the procedure above to the problem at hand, let $y_m^*$ be the value of $y^*$ at which $T = T_m$ ; remembering that $y_m^*$ is always a large number we find, from Eq. (3.8):

$$\frac{\rho c_p u_\tau}{q_o}(T_m - T_i) = \frac{1}{\sqrt{K}} \ln y_m^* - \frac{1}{\sqrt{K}} \ln\left(y_i^* + \frac{2-\sigma}{2\sqrt{K\sigma}}\right) + O\left(\frac{1}{y_m^*}\right) \qquad (3.9)$$

where the order of the terms neglected is indicated. If the dimensionless mean velocity $u_m^*$ occurs at $y_m^*$ as well, then from Eq. (2.3):

$$u_m^* = \frac{1}{\sqrt{K}} \ln y_m^* + B \qquad (3.10)$$

Subtracting (3.10) from (3.9), and multiplying through by $u_m^* = u_m/u_\tau$ :

$$\frac{\rho c_p u_\tau}{q_o}(T_m - T_i) = (u_m^*)^2 - \left[\frac{1}{\sqrt{K}} \ln\left(y_i^* + \frac{2-\sigma}{2\sqrt{K\sigma}}\right) + B\right] u_m^* \qquad (3.11)$$

Putting $y^* = y_1^*$ in the expressions (3.6) or (3.7) and multiplying through by $u_m^*$ , an expression for $\frac{\rho c_p u_\tau}{q_o}(T_i - T_w)$ is obtained. Adding this to (3.11) and defining the heat transfer coefficient $C_h$ as:

$$C_h = \frac{q_o}{\rho c_p u_m (T_m - T_w)} \qquad (3.12)$$

we obtain an equation for $C_h$ in the form:

$$\frac{1}{C_h} = \frac{2}{C_f} + F(\sigma)\sqrt{\frac{2}{C_f}} \qquad (3.13)$$

where by definition, $u_m^* = u_m/u_\tau = \sqrt{\rho u_m^2/\tau_o} = \sqrt{2/C_f}$ and the function $F(\sigma)$ is:

$$F(\sigma) = \frac{\sigma}{\sqrt{K_i}\sqrt{1-\sigma}} \tanh^{-1}\left(\sqrt{1-\sigma}\tanh\sqrt{K_i}\, y_i^*\right) - B - \frac{1}{\sqrt{K}} \ln\left(y_i^* + \frac{2-\sigma}{2\sqrt{K\sigma}}\right) \qquad \sigma < 1 \qquad (3.14)$$

$$= \frac{\sigma}{\sqrt{K_i}\sqrt{\sigma-1}} \tan^{-1}\left(\sqrt{\sigma-1}\tanh\sqrt{K_i}\, y_i^*\right) - B - \frac{1}{\sqrt{K}} \ln\left(y_i^* + \frac{2-\sigma}{2\sqrt{K\sigma}}\right) \qquad \sigma > 1 \qquad (3.15)$$

It will be noticed that the form of Eq. (3.13) is exactly the same as that of Prandtl (1.11) and Kármán (1.18) but the function $F(\sigma)$ is different in each.

Before discussing these results in detail, other methods of defining the mean temperature should be examined. The mean temperature is sometimes identified with the average temperature over the pipe cross-section, but a more common definition is the average over the pipe of the temperature weighted with the velocity ratio $u/u_m$, where $u_m$ is the mean velocity. This latter definition corresponds to the temperature obtained if the fluid is completely mixed, and in many heat transfer experiments the mean temperature is measured most conveniently in this way.

The average velocity over the pipe cross-section is, in dimensionless form:

$$u_m^* = \frac{2}{R^{*2}} \int_0^{R^*} u^* (R^* - y^*) \, dy^* \tag{3.16}$$

where $R^*$ is a dimensionless radius defined as:

$$R^* = \frac{R u_\tau}{\nu} = \frac{1}{2} \sqrt{\frac{c_f}{2}} \, R_e \tag{3.17}$$

and $R_e$ is the Reynolds number $2R u_m/\nu$. The mean velocity $u_m^*$ can be determined from (3.16) by substituting the expressions for $u^*$ from (2.3) and (2.10) into the integral and evaluating. The thickness of the wall layer $y_1^*$ is small compared with $R^*$, particularly at larger Reynolds numbers and hence the core gives the most important contribution to the integral. Retaining only the largest terms:

$$u_m^* = \frac{2}{R^{*2}} \int_0^{R^*} \left( \frac{1}{\sqrt{k}} \ln y^* + B \right) (R^* - y^*) \, dy^* + O\left(\frac{1}{R^*}\right) \tag{3.18}$$

The terms of order $1/R^*$ are negligible at large Reynolds numbers and small, although scarcely negligible, at a Reynolds number of 10,000.

It is doubtful, however, that any accuracy would be gained by evaluating these terms at the smaller Reynolds number. As was pointed out previously, the approximation of replacing $\tau = \tau_0(1 - y/R)$ by $\tau_0$ becomes less sound at $R_e = 10{,}000$ or so, and the errors introduced may well be of the same order of magnitude as the terms neglected in (3.18). The momentum and energy transfer in the range of Reynolds number between 2,000 and 10,000 requires more elaborate investigation, and this will not be attempted here.

The integration of (3.18) is quite simple and leads to the result:

$$u_m^* = \frac{1}{\sqrt{K}} \ln R^* + B - \frac{3}{2\sqrt{K}} \tag{3.19}$$

Since $u_m^* = \sqrt{2/C_f}$, a useful equation for the friction coefficient can be derived from (3.17) and (3.19) in the form:

$$\sqrt{\frac{2}{C_f}} = \frac{1}{\sqrt{K}} \ln R_e - \frac{1}{\sqrt{K}} \ln \sqrt{\frac{2}{C_f}} - \frac{1}{\sqrt{K}} \ln 2 + B - \frac{3}{2\sqrt{K}} \tag{3.20}$$

or substituting the numerical values (2.5) for B and K :

$$\sqrt{\frac{2}{C_f}} = 2.5 \ln R_e - 2.5 \ln \sqrt{\frac{2}{C_f}} \tag{3.21}$$

This is very nearly the same as a formula derived by Kármán in different way, which, in our notation becomes:

$$\sqrt{\frac{2}{C_f}} = 2.46 \ln R_e - 2.46 \ln \sqrt{\frac{2}{C_f}} + 0.30$$

These relations for the friction coefficient will be useful later. Returning to the evaluation of the weighted mean temperature, we define $T_m$ as:

$$T_m - T_w = \frac{2}{R^{*2} u_m^*} \int_0^{R^*} (T - T_w)\, u^* (R^* - y^*)\, dy^* \tag{3.22}$$

In dimensionless form this expression is the same as:

$$\frac{1}{C_h} = \frac{\rho c_p u_m (T_m - T_w)}{q_o} = \frac{2}{R^{*2}} \int_0^{R^*} \frac{\rho c_p u_r}{q_o} (T - T_w)\, u^* (R^* - y^*)\, dy^* \qquad (3.23)$$

Introducing the expressions for the velocity (2.3) and the temperature (3.8) and neglecting terms of order $1/R^*$ as before:

$$\frac{1}{C_h} = \frac{2}{R^{*2}} \int_0^{R^*} \frac{1}{\sqrt{K}} \ln y^* \left(\frac{1}{\sqrt{K}} \ln y^* + B\right)(R^* - y^*)\, dy^* + \left[\frac{\rho c_p u_r}{q_o}(T_1 - T_w) - \frac{1}{\sqrt{K}} \ln\left(y_1^* + \frac{2-\sigma}{2\sqrt{K}\sigma}\right)\right] u_m^*$$

The integral is easily evaluated, and if the terms in $\ln R^*$ are eliminated by substitution from (3.19) we find:

$$\frac{1}{C_h} = \frac{2}{C_f} + F(\sigma)\sqrt{\frac{2}{C_f}} + \frac{5}{4K} \qquad (3.24)$$

This equation is the same as (3.13) except for the added constant. The constant $5/4K = 7.81$ is a relatively small correction if $\sigma > 1$ since the term $2/C_f$ will not be less than 200 for smooth pipes.

The factor $F(\sigma)$ derived above is a function of $\sigma$ alone and introducing the values of B, K, y1* and K1 from (2.5) and (2.16):

$$F(\sigma) = 14.53 \frac{\sigma}{\sqrt{1-\sigma}} \tanh^{-1}\left(0.955\sqrt{1-\sigma}\right) - 5.5 - 2.5 \ln\left(26.3 + \frac{2.5}{\sigma}\right) \qquad \sigma < 1 \qquad (3.25)$$

$$= 14.53 \frac{\sigma}{\sqrt{\sigma-1}} \tan^{-1}\left(0.955\sqrt{\sigma-1}\right) - 5.5 - 2.5 \ln\left(26.3 + \frac{2.5}{\sigma}\right) \qquad \sigma > 1 \qquad (3.26)$$

A plot of $F(\sigma)$ is shown in Fig. 2, together with the corresponding expression found by Kármán, (1.18):

$$5\left[(\sigma - 1) + \ln\{1 + 0.83(\sigma - 1)\}\right]$$

The two expressions agree for $0.1 < \sigma < 10$, as is to be expected, but the difference becomes very large for $\sigma > 50$. The behavior of $F(\sigma)$ for

extreme values of $\sigma$ can be seen from (3.14) and (3.15) to be:

$$F(\sigma) \to -\frac{1}{\sqrt{K}}\ln\frac{1}{\sigma} - \frac{1}{\sqrt{K}}\ln\frac{1}{\sqrt{K}} - B \qquad = -2.5\ln\frac{1}{\sigma} - 7.8 \quad (\sigma \to 0) \quad (3.27)$$

$$F(\sigma) \to \frac{\pi}{2}\frac{\sqrt{\sigma}}{\sqrt{K_1}} - B - \frac{1}{\sqrt{K_1}\tanh\sqrt{K_1}y_1^*} - \frac{1}{\sqrt{K}}\ln y_1^* = 22.8\sqrt{\sigma} - 29.1 \quad (\sigma \to \infty) \quad (3.28)$$

whereas the corresponding function of Kármán behaves quite differently, approaching $-14$ as $\sigma \to 0$ and $5\sigma$ as $\sigma \to \infty$. Although the analysis given here takes into account the conduction of heat in the part of the turbulent core nearest the wall, and should represent an improvement over Kármán's analysis for small Prandtl numbers, neither theory will be satisfactory at extremely small values of $\sigma$. For these it is necessary to take into account the correct form of the heat flux; i.e., $q_0(1 - y/R)$ rather than $q_0$ as used here. There is no difficulty in doing this, but since the turbulent transport of heat in the wall layer is relatively unimportant when $\sigma$ is very small, the result should not differ appreciably from that of Martinelli, (Ref. 9), who used the Kármán approximation for the velocity profile at the wall.

The effect of varying the Prandtl number over a wide range, keeping the Reynolds number constant, is to change the relative proportions of turbulent and molecular transports of energy at any given distance from the wall, without changing the proportions of the momentum transports. In principle at least, it should be possible to deduce, from overall heat transfer measurements at various Prandtl numbers, the proportions of turbulent and molecular transports at all distances from the wall. In practice it is difficult to do this accurately because of scatter in

heat transfer data. The simplest procedure is to guess at a law for the turbulent transport of energy, calculate the heat transfer rate as a function of Prandtl number and compare with experiment. This is the procedure used here essentially, although the initial guess was derived from momentum transport and has been confirmed to some extent already.

The heat transfer measurements, in spite of inaccuracies comprise much more sensitive tests of the validity of the assumed transport laws than the velocity profile measurements. The magnitude of the turbulent transport very close to the wall, from $y^* = 1$ to $y^* = 10$ say, can be determined much more accurately from heat transfer data for fluids with Prandtl numbers between 1 and 100 than from direct velocity measurements. Similarly, the turbulent transport in the part of the wall layer near the core could be investigated through heat transfer measurements for fluids with Prandtl numbers ranging from 1 down to 0.01. No such fluids seem to exist, however, so this method of exploring the outer part of the wall layer is not available. This means, of course, that accurate evaluation of the energy transport in that region is not essential, because situations where it is important will not arise in practice.

A comparison of the calculated values of the Nusselt number $N_u = C_h R_e \sigma$ with measurements of several observers is shown in Fig. 3. The data, representing typical results, were taken from Ref. 14, page 168 and all are reported for a pipe Reynolds number of 10,000. In evaluating $C_h$ from Eq. (3.13), the empirical friction formula $C_f = 0.046/R_e^{0.2}$ was used, giving in this case $C_f = 0.0073$. The agreement is excellent over the entire Prandtl number range, whereas

Kármán's formula gives only half the experimentally observed heat transfer coefficient at $\sigma = 100$. A widely used empirical formula for this range of Prandtl numbers is (Ref. 14, p. 168):

$$N_u = 0.023 (R_e)^{0.8} \sigma^{0.4}$$

On page 181 of Ref. 14, a large number of heat transfer measurements are plotted on a logarithmic chart of $N_u/\sigma^{0.4}$ vs. $R_e$. The Prandtl numbers of the fluids ranged from 3 to 33 and if the empirical formula above were correct, all test data should lie on a single straight line. There is considerable deviation from the line and this is ascribed to scatter. Certainly the scatter is large but there appears to be a discernable, although not well-marked, trend with Prandtl number. If $N_u$ is calculated from the $C_h$ in (3.24) and $N_u/\sigma^{0.4}$ plotted vs. $R_e$, the lines of constant $\sigma$ are almost straight, almost parallel, and quite close together for $1 < \sigma < 100$ say. The experimental points for various Prandtl number groups seem to follow the trend predicted by the theory. The scatter is so large that one can scarcely draw a definite conclusion; the main point is that the theory given here agrees as well, and probably better, with the experiments than the widely used empirical formula above.

The agreement of the theory with experiment shows that the turbulent transport law assumed here cannot be far wrong. At very high Prandtl numbers, the theory shows that $C_h \cong \frac{2}{\pi} \frac{\sqrt{K_1}}{\sqrt{\sigma}} \sqrt{\frac{C_f}{2}}$, as can be seen from Eqs. (3.13) and (3.28), and hence the variation with $\sigma$ must be essentially correct. Even more remarkable, the value of $K_1$, which was determined from the empirical constants in the velocity

profile equation for the core, must be about right. At least, there seems to be no reason for changing it.

It is interesting to note that the analysis above can be applied to mass transfer merely by changing notation. If c is the concentration of one fluid diffusing into another fluid from the wall of a pipe, and if the concentration gradient along the pipe is small compared with the gradient normal to the wall, the rate of transport of mass normal to the wall per unit area is:

$$m_o = -\overline{c'v'} + D\frac{dc}{dy} \tag{3.30}$$

The quantity D is the coefficient of diffusion resulting from molecular transport. This equation can be rewritten in the form:

$$m_o = \left[-\frac{\overline{c'v'}}{dc/dy} + \frac{\nu}{S_c}\right]\frac{dc}{dy} \tag{3.31}$$

where $S_c = \nu/D$ , the Schmidt number. Applying the Reynolds analogy to the turbulent transport term:

$$\frac{\overline{c'v'}}{dc/dy} = \frac{\overline{u'v'}}{du/dy}$$

Eq. (3.31) can be treated in a fashion identical with that used for the energy equation. Defining the mass transfer coefficient as $C_c = m_o/u_m(c_m - c_w)$, where $C_m$ is the mean concentration over the pipe and $C_w$ is the concentration at the wall, one finds:

$$\frac{1}{C_c} = \frac{2}{C_f} + F(S_c)\sqrt{\frac{2}{C_f}} + 7.8 \tag{3.32}$$

where F is given by (3.25) and (3.26) with $\sigma$ replaced by $S_c$ . The Schmidt number for water vapor diffusing into air is 0.49 and some other

combinations of gases have Schmidt numbers ranging from 0.1 to 1.0. This same range of Prandtl numbers is not well covered in heat transfer, hence there would be considerable advantage in testing the validity of the assumed transport mechanism by mass transfer measurements.

There is one assumption about which some question still remains - the Reynolds analogy. If a "turbulent Prandtl number" $\sigma_t$ exists and if it is constant, it can be included in the analysis without difficulty. It is merely necessary to introduce the factor $\sigma_t$ multiplying the turbulent transport terms in the denominators of Eqs. (3.4) and (3.5). Multiplying numerators and denominators by $\sigma_t$, it is clear that the effect on (3.13) is simply to change this to:

$$\frac{1}{C_h} = \sigma_t \left[ \frac{2}{C_f} + F\left(\frac{\sigma}{\sigma_t}\right)\sqrt{\frac{2}{C_f}} \right] \tag{3.29}$$

If $\sigma_t \cong 0.75$, as suggested by several independent investigators, then for air where $\sigma \cong 0.75$, $F(\sigma/\sigma_t) = 0$ and $C_h \cong 1.3\, C_f/2$. This last relation gives poorer agreement with heat transfer measurements on air in pipes than if $\sigma_t = 1$. Hence for pipe flow it appears that the Reynolds analogy must be very nearly true, at least in the regions close to the wall.

To summarize the findings in this section, heat transfer coefficients have been determined in a form convenient for applications. The results agree closely with experiment at high Prandtl numbers, where empirical laws only have been available heretofore. The agreement shows that the forms of the velocity profile and the turbulent transports of momentum and energy must be essentially correct in the region very close to the wall.

## IV. MOMENTUM TRANSPORT WITH VARIABLE VISCOSITY

The viscosities of liquids are rather sensitive functions of temperature and large variations can occur at high rates of heat transfer. The most rapid change of temperature is found at the wall, and because most liquids have Prandtl numbers higher than unity, most of the temperature variation, and hence the viscosity variation, occurs within the wall layer. So far, no theory for heat transfer with variable viscosity has appeared, although a number of empirical formulae that are more or less satisfactory over restricted ranges of the variables have been employed. Experimental data have, in the past, been rather unreliable and it has been difficult to find ways in which a theory could be tested with confidence. More recently experimental techniques have improved, mostly as a result of increased interest in high rates of heat transfer. The availability of these data together with the success of the analysis above for isothermal flow gives encouragement to attempt extending the theory to the more complex phenomena arising from variable viscosity.

The momentum equation for pipe flow with variable viscosity is the same as Eq. (2.1) and for distances from the wall small compared with the pipe radius becomes:

$$\frac{\tau_0}{\rho} = u_\tau^2 = -\overline{u'v'} + \frac{\mu}{\rho}\frac{du}{dy} \tag{4.1}$$

where it will be assumed that $\rho$ is constant. The viscosity $\mu$ is primarily a function of temperature and hence the momentum and energy equations are coupled and must be solved simultaneously. In order to

make the problem manageable, it will be assumed that $\mu$ is a given function of $y$, the distance from the wall. In this way the momentum equation can be solved independently of the energy equation. Such a procedure does not avoid the difficulty of the coupling of course, because eventually this must be introduced, but it simplifies solution of the momentum equation, and the latter is the key to the solution of the energy equation. One further assumption will be made, and this introduces a definite restriction: the viscosity variation takes place almost entirely within the wall layer. Hence the final solution will apply only to liquids with Prandt numbers greater than unity, where the most of the temperature difference occurs in the wall layer and very little in the core. Fortunately, all liquids other than metallic liquids do have Prandtl numbers greater than unity. Gases, however, aside from the complication of variable density, are excluded becausefifty percent or so of the temperature difference and hence of the viscosity variation occurs in the turbulent core.

With the assumption that the viscosity varies in the wall layer only, we introduce the notation:

$$\frac{\mu}{\mu_1} = f(y^*) \qquad f(0) = \frac{\mu_w}{\mu_1} \qquad f(y^*) \cong 1 \quad \text{for} \quad y^* > y_1^* \tag{4.2}$$

where $y^* = y u_\tau/\nu_1$ , $\mu_1$ is the viscosity at $y1^*$ and $\mu_w$ the viscosity at the wall, $y1^*$ being the edge of the wall layer as before. It is assumed that $\mu_1$ is not much different from $\mu_m$. Eq. (4.1) can be written in dimensionless form as:

$$1 = -\frac{\overline{u'v'}}{u_\tau^2} + f(y^*)\frac{du^*}{dy^*} \tag{4.3}$$

where $u^* = u/u_\tau$ as defined previously. Because the assumption $-\overline{u'v'} = K_1 u^2$ for the turbulent shear stress worked so successfully before, it is tempting to try it here. This is quite wrong, however, as it assumes a certain type of local similarity for which there is no justification. In spite of its incorrectness, the solution of (4.3) with this assumption is illuminating because it represents an extreme; the solution is easily found to be:

$$u^* = \frac{1}{\sqrt{K_1}} \tanh\left(\sqrt{K_1}\, Y^*\right)$$

where

$$Y^* = \int_0^{y^*} \frac{dy^*}{f(y^*)} \qquad (4.4)$$

The function $Y^*(y^*)$ replaces $y^*$ in the corresponding solution for constant viscosity, i.e. (2.10), and represents a modified distance from the wall that takes into account the viscosity variation.

The turbulent shear stress that results from the assumption above is given by:

$$-\frac{\overline{u'v'}}{u_\tau^2} = \tanh^2\left(\sqrt{K_1}\, Y^*\right) \qquad (4.5)$$

Very close to the wall this approaches $K_1 Y^{*2}$ which in turn approaches $K_1 \left(\frac{\mu_1}{\mu_w} y^*\right)^2$ as $y^*$ goes to zero. Hence the turbulent shear stress immediately adjacent to the wall is increased over that for constant viscosity by the factor $(\mu_1/\mu_w)^2$ and is therefore the same as if the viscosity were $\mu_w$ throughout the pipe. Intuitively it seems unlikely that this could be true; if the friction and heat transfer coefficients are calculated from (4.5) with $\mu_w < \mu_1$, for instance, they turn out to

be too large, showing that the assumption above overestimates the turbulent transport in this case.

As the other extreme, one might assume the alternative expression for the turbulent shear stress from the solution for constant viscosity, and put:

$$-\frac{\overline{u'v'}}{u_\tau^2} = \tanh^2(\sqrt{K}\,y^*) \qquad (4.6)$$

which implies that the turbulent transport is unaffected by the variation of viscosity in the wall layer. This is quite wrong too, and if $\mu_w < \mu_1$ the friction and heat transfer coefficients calculated on this basis are much too low, showing that (4.6) underestimates the turbulent shear stress. The correct distribution of the turbulent shear stress must lie between (4.5) and (4.6) and it is clear that no simple similarity law can give it.

The source of velocity fluctuations in turbulent flow in a pipe is in the core and outer part of the wall layer next the core. Laufer (Ref. 11) found the velocity fluctuations to reach a maximum within the outer third of the wall layer next the core. The inner part of the wall layer, next the wall, must be very stable and any velocity fluctuations within this region will not arise there but consist of forced oscillations coming from outside, presumably from the outer third of the wall layer mainly. The part of the wall layer next the wall is primarily a region of damping. If this picture is correct, the influence of variable viscosity on turbulent transport can be clarified. Suppose, for example, that the viscosity is least at the wall and

increases monotonically toward the core. The velocity fluxtuations, and hence the turbulent shear stress, very close to the wall must be influenced by the presence of the stable region of higher viscosity between the wall region and the source of the fluctuations further out. The assumption leading to the expression (4.5) for the turbulent shear stress does not take into account the region of higher viscosity which the velocity fluctuations must penetrate before reaching the wall. As a result the shear stress is too high. The alternative assumption (4.6) is correct in the outer part of the wall layer but neglects the effect of the lower viscosity very close to the wall which allows the fluctuations to last longer and hence produce a larger turbulent shear stress. If the influence of variable viscosity is to be estimated, the entire path of the velocity fluctuations from their source down to the wall must be taken into account.

The picture described above suggests a simple idealized model for the part of the wall layer that is essentially a damping region. Imagine a fluid contained by two parallel walls, one fixed and the other oscillating in its plane with a sinusoidal motion. The equation of motion for the fluid is $\rho \partial u/\partial t = \frac{\partial}{\partial y}\left(\mu \frac{\partial u}{\partial y}\right)$ and putting $u = U(y)\, e^{i\omega t}$ and $\mu = \mu_1 f(y)$, the amplitude equation is:

$$\frac{d}{dy}\left(f \frac{dU}{dy}\right) - i \frac{\omega}{\nu_1} U = 0 \qquad (4.7)$$

with boundary conditions:

$$U = 0 \quad \text{at} \quad y = 0 \qquad\qquad U = U_b \quad \text{at} \quad y = b$$

if the distance between the walls is $b$. For constant viscosity, $f = 1$ say, the velocity amplitude at any value of $y$ is easily shown to be given by:

$$|U/U_b| = \left[ \frac{\cosh \beta y/b - \cos \beta y/b}{\cosh \beta - \cos \beta} \right]^{1/2}$$

where $\beta = b\sqrt{\omega/2\nu_1}$ . The approximate shapes of the amplitude curves for various values of the frequency parameter $\beta$ are sketched on the left.

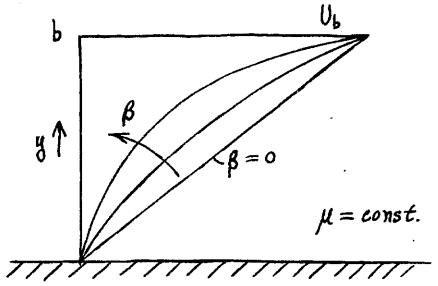


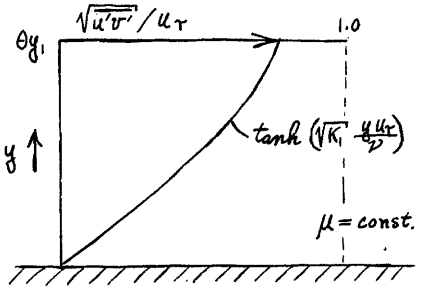


This model probably gives a good representation of $u'$ in the region very close to the wall in turbulent flow if $b$ is identified with the distance of the source of oscillations from the wall. No such simple representation of $v'$ can be devised but it seems reasonable to assume that $v'$ behaves in about the same way as $u'$ . The actual velocity fluctuations in the wall layer will cover a spectrum of frequencies and this spectrum will undoubtedly change with distance from the wall. Since it is assumed that $v'$ behaves like $u'$ , then $\sqrt{\overline{u'v'}}$ should behave like $u'$ , and the most logical way of choosing the frequency is to match the known turbulent shear stress with one of the curves above. The shape of $\sqrt{\overline{u'v'}}$ is shown on the right, where $\theta y_1$ is the

thickness of the region of damping near the wall. The factor $\theta$ will be of the order of 0.7 or so. The shape of the shear stress curve does not match any one of the curves on the left. The region very close to the wall is most important, however, because the most rapid change of viscosity occurs there, and if one compromises on the outer region, the zero frequency curve fits best, since $\tanh(\sqrt{K_1}\, y u_\tau/\nu)$ starts off as a straight line. This identification is quite reasonable because it is clear that only the very low frequency fluctuations can penetrate to the wall; the higher frequencies will be damped out before they reach the region very close to the wall.

If low frequency fluctuations only are of interest, the solution of the problem in the idealized model for variable viscosity becomes extremely simple. Putting $\omega = 0$ in Eq. (4.7), the velocity amplitude for any viscosity variation is given by:

$$U/U_{\theta y_1} = \int_0^y \frac{dy}{f(y)} \Big/ \int_0^{\theta y_1} \frac{dy}{f(y)}$$

where b is identified with $\theta y_1$. Introducing the dimensionless variable $y^* = y u_\tau/\nu_1$ this equation is identical with:

$$U/U_{\theta y_1} = Y^*(y^*)/Y^*(\theta y_1^*) \qquad (4.8)$$

where Y* is the modified distance from the wall defined by (4.4). For constant viscosity, the corresponding zero frequency equation was $U/U_{\theta y_1} = y^*/\theta y_1^*$ and hence the amplification factor resulting from variable viscosity is $\theta y_1^* Y^*/y^* Y^*_{\theta y_1}$. The numerical value to be assigned to $\theta$ is somewhat in doubt. Laufer's measurements (Ref. 11)

indicate that the value of $y$ at which the $u'$ fluctuations reach a maximum moves out toward the edge of the wall layer as the Reynolds number increases. It seems sufficiently accurate to put $\theta \equiv 1$ in the amplification factor above, although this overestimates the factor slightly. Any further refinement is scarcely justifiable in view of the approximate nature of the calculation. With $\theta = 1$, the magnification factor is simply $y_1^* \Upsilon^* / y^* \Upsilon_1^*$.

The turbulent shear stress very close to the wall should be increased by the square of the amplification factor and since $-\overline{u'v'}/u_\tau^2 = \tanh^2(\sqrt{K_1}\, y^*)$ for constant viscosity, the corresponding expression for variable viscosity will be assumed to be:

$$-\frac{\overline{u'v'}}{u_\tau^2} = \tanh^2\left(\sqrt{K_1}\,\frac{y_1^*}{\Upsilon_1^*}\,\Upsilon^*\right) = \tanh^2\left(\sqrt{K_1'}\,\Upsilon^*\right) \tag{4.9}$$

where

$$\sqrt{K_1'} = \sqrt{K_1}\, y_1^*/\Upsilon_1^* \tag{4.10}$$

The amplification factor is introduced into the argument of the hyperbolic tangent rather than multiplying the function itself; hence it is applied correctly very close to the wall, but only approximately further out. The turbulent shear stress must approach $\tau_0$ at the outer edge of the wall layer where the laminar shear stress becomes negligible, and the way in which the correction for variable viscosity was introduced guarantees this, as can be seen from (4.9). The calculation of the turbulent shear stress involves two rather drastic approximations. One of these, the restriction to zero frequency oscillations, is correct very close to the wall but not further out in the wall

layer where the higher frequencies become important. The other approximation, the method of modifying the shear stress for variable viscosity, is also probably valid very close to the wall but not further out. However, the final expression for the turbulent shear stress must be about right in the outer part of the wall layer and it is clear that errors introduced by the approximations tend to compensate each other. There is no way of determining the accuracy of the expression (4.9) for the turbulent shear stress, but it is not impossible that it is very close to reality.

Substituting the expression (4.9) into Eq. (4.3), the velocity profile is found by simple integration to be:

$$u^* = \frac{1}{\sqrt{K_1'}} \tanh\left(\sqrt{K_1'}\, Y^*\right) \tag{4.11}$$

and the velocity gradient is:

$$\frac{du^*}{dy^*} = \frac{1}{f(y^*)} \operatorname{sech}^2\left(\sqrt{K_1'}\, Y^*\right) \tag{4.12}$$

Both of these expressions reduce to the isothermal forms (2.10) and (2.13) when $f(y^*) \equiv 1$. The velocity profile in the turbulent core is assumed to be the same as if the viscosity were $\mu_1$, constant throughout the flow. Then the expression (2.11) for the velocity gradient still applies. Equating the two expressions for the velocity gradient; i.e., (2.11) and (4.12) at $y^* = y1^*$ and making use of the relations $f(y_1^*) = 1$ and $\sqrt{K_1'}\, Y_1^* = \sqrt{K_1}\, y_1^*$, we have:

$$\operatorname{sech}^2\left(\sqrt{K_1}\, y_1^*\right) = \frac{1}{\sqrt{K}\, y_1^*} - \frac{1}{2K y_1^{*2}}$$

This equation is identical with (2.15) for isothermal flow and $K$ and $K_1$ are the same, hence $y_1^* = 27.5$ as before. The thickness of the wall layer does not change with variation of viscosity provided that this variation is confined to the part of the wall layer closest to the wall.

The velocity profile is found, as before, by integrating Eq. (2.11) giving:

$$u^* = \frac{1}{\sqrt{K}} \ln y^* + B' + \frac{1}{2Ky^*} \tag{4.13}$$

where a new constant $B'$ is introduced instead of $B$, which in isothermal flow was found to be 5.5 from experiment. The constant $B'$ is found by joining (4.11) to (4.13) at $y^* = y_1^*$ :

$$B' = \frac{1}{\sqrt{K_1'}} \tanh\left(\sqrt{K_1'}\, Y_1^*\right) - \frac{1}{\sqrt{K}} \ln y_1^* - \frac{1}{2Ky_1^*}$$

or, making use of Eqs. (2.14) and (4.10):

$$B' = \left(\frac{Y_1^*}{y_1^*} - 1\right) \frac{1}{\sqrt{K_1}} \tanh\left(\sqrt{K_1}\, y_1^*\right) + B \tag{4.14}$$

Introducing the numerical values for $K_1$ and $y_1^*$ from (2.16) and putting $B = 5.5$:

$$B' = 13.89\, Y_1^*/y_1^* - 8.39 \tag{4.15}$$

From the definition of $Y^*$ it can be seen that if the viscosity in the wall layer is less than in the core, $B'$ is greater than 5.5 and the average velocity through the pipe is larger than for viscosity in the

wall layer equal to that in the core; the reverse holds for viscosity at the wall larger than in the core.

The constancy of the wall layer thickness is not unreasonable and it is consistent with the picture of the way in which the velocity fluctuations arise and are damped close to the wall. If the viscosity is decreased in the damping region close to the wall, but remains constant throughout the core and the regions in which the fluctuations arise, the velocity gradient will be the same as for isothermal flow except in the region close to the wall. In this latter region, the velocity profile changes, giving rise to an increase of the core velocity if the pressure drop and shear stress are kept the same. The change of velocity profile close to the wall does not affect the core by introducing any velocity fluctuations because this is a damping region. The self-induced turbulent fluctuations further out from the wall are related to the velocity gradient, not the velocity, and the gradient is the same as before. The velocity and velocity gradient must be continuous at the junction of the damped and unstable regions and the core velocity is increased because of the changes in the region close to the wall. This increase of the core velocity is the sole effect on the core of the decrease in viscosity close to the wall. The laminar and turbulent shear stresses next the wall are both modified by the decrease of viscosity although the total shear stress remains the same. The method of calculation of the influence of variable viscosity is valid only if most of the variation is confined to the region very close to the wall. If an appreciable change of

viscosity takes place over the region in which the velocity fluctuations arise, the description of the velocity profile taken from isothermal flow will not apply. The effect of variable viscosity in the turbulent region on the transport of momentum is not yet known.

The average velocity over the pipe cross section is given by Eq. (3.16) with the new expressions for $u^*$ from (4.11) and (4.13). Neglecting terms of order $1/R^*$ as before, we find:

$$u_m^* = \frac{1}{\sqrt{K}} \ln R^* + B' - \frac{3}{2K} \tag{4.16}$$

instead of Eq. (3.19). Substituting numerical values and re-arranging, an equation for the friction coefficient is obtained in the form:

$$\sqrt{\frac{2}{C_f}} = 2.5 \ln R_e - 2.5 \ln \sqrt{\frac{2}{C_f}} + 13.89 \left( \frac{Y_1^*}{y_1^*} - 1 \right) \tag{4.17}$$

where the Reynolds number $R_e$ is defined in terms of the viscosity . The friction coefficient is influenced by variable viscosity only through the ratio $Y_1^*/y_1^*$ , at least for Reynolds numbers above 10,000. In the various empirical formulas that have been developed for the friction coefficient, it always has been assumed that the effect of variable viscosity could be correlated with some viscosity ratio, $\mu_m/\mu_w$ say, alone. According to the theory developed here, the effect is more complicated, because the ratio $Y_1^*/y_1^*$ depends not only on the viscosity ratio, but also the shape of the curve of viscosity versus $y^*$ . The value of $Y_1^*$ depends on how rapidly the viscosity change near the wall takes place.

This completes the analysis of the momentum transfer for variable viscosity. There is no way of proving that the details of the mechanism postulated here are correct; confidence in their validity can be gained only if the predicted friction and heat transfer coefficients agree well with experiment. The comparison with measurements will be made after the analysis of the energy transfer in the section following.

## V. ENERGY TRANSFER WITH VARIABLE PHYSICAL PROPERTIES

When the density is constant, the energy equation for variable specific heat and conductivity is:

$$q_o = -\rho \overline{h'v'} + k \frac{dT}{dy} \tag{5.1}$$

where $h$ is the enthalpy, defined as:

$$h = \int c_p \, dT \tag{5.2}$$

The properties $C_p$ and $k$ are assumed to be functions of temperature only. The energy equation can be rewritten as:

$$q_o = \rho \left[ - \frac{\overline{h'v'}}{dh/dy} + k \frac{dT}{dh} \right] \frac{dh}{dy} \tag{5.3}$$

and applying the Reynolds analogy to the transport of enthalpy:

$$\frac{\overline{h'v'}}{dh/dy} = \frac{\overline{u'v'}}{du/dy}$$

the energy equation becomes:

$$q_o = \rho \left[ - c_p \frac{\overline{u'v'}}{du/dy} + k \right] \frac{dT}{dy}$$

Introducing $C_{p1}$ and $k_1$, the values of these quantities at $y_1^*$ and expressing in dimensionless form in terms of $y^* = y u_\tau / \nu_1$, this equation can be written:

$$\frac{\rho c_p u_\tau}{q_o} \frac{dT}{dy^*} = \frac{1}{- \frac{c_p}{c_{p_1}} \frac{\overline{u'v'}/u_\tau^2}{du^*/dy^*} + \frac{k}{k_1} \frac{1}{\sigma_1}} \tag{5.4}$$

where $\sigma_1$ is the Prandtl number at $y_1^*$. This equation reduces to Eq. (3.3) when the physical properties are constant.

The expressions (4.9) and (4.12) for $\overline{u'v'}/u_\tau^2$ and $du^*/dy^*$ derived in the preceding section for variable viscosity can be substituted into (5.4) to give the temperature profile in the wall layer:

$$\frac{\rho c_p u_\tau}{q_0}(T-T_w) = \int_0^{y^*} \frac{dy^*}{\frac{c_p}{c_{p_1}} f \sinh^2(\sqrt{K'}Y^*) + \frac{k}{k_1}\frac{1}{\sigma_1}} \qquad 0<y^*<y_1^* \qquad (5.5)$$

In the turbulent core, it will be assumed that the physical properties are constant, their values being the same as at $y_1^*$. This assumption introduces some error but the error should be small if most of the temperature difference is confined to the wall layer. The temperature profile for the core is then, from Eq. (3.8):

$$\frac{\rho c_p u_\tau}{q_0}(T-T_1) = \frac{1}{\sqrt{K'}} \ln \frac{y^* + \frac{2-\sigma_1}{2\sqrt{K'}\sigma_1}}{y_1^* + \frac{2-\sigma_1}{2\sqrt{K'}\sigma_1}} \qquad y^* > y_1^* \qquad (5.6)$$

The mean temperature can be found by either of the two methods given in Section III. The equation for the heat transfer coefficient corresponding to Eq. (3.24) is:

$$\frac{\rho c_{p_1} u_m (T_m - T_w)}{q_0} = \frac{1}{C_h} = \frac{2}{C_f} + F\sqrt{\frac{2}{C_f}} + \frac{5}{4K} \qquad (5.7)$$

where

$$F = \int_0^{y_1^*} \frac{dy^*}{\frac{c_p}{c_{p_1}} f \sinh^2(\sqrt{K'}Y^*) + \frac{k}{k_1}\frac{1}{\sigma_1}} - B' - \frac{1}{\sqrt{K'}} \ln\left(y_1^* + \frac{2-\sigma_1}{2\sqrt{K'}\sigma_1}\right) \qquad (5.8)$$

and $C_f$ is given by Eq. (4.17).

The expressions above represent the complete solution of the heat transfer problem. In practice a method of successive approximations must be applied because $\mu$ , $C_p$ and $k$ will be given functions of the temperature $T$ rather than of $y^*$ as is required in the integrals. The procedure will depend to some extent on the way in which the problem is stated, but the method suggested below is the one that will be used in the comparison with experiment. Suppose that the mean temperature $T_m$ and the wall temperature $T_w$ are given, as well as the Reynolds number $Re_m$ based on mean properties. The properties $\mu$ , $C_p$ and $k$ are known functions of $T$. The first step is to guess at the variation of $f = \mu/\mu_1$ as a function of $y^*$. The viscosity $\mu_1$ at $y_1^*$ can be identified with $\mu_m$ initially if desired. From the estimated variation of $f$ , $Y^*$ can be determined as a function of $y^*$ from:

$$Y^* = \int_0^{y^*} \frac{dy^*}{f}$$

Then $\sqrt{K_1'} = \sqrt{K}\, y_1^*/Y_1^* = 0.069\, y_1^*/Y_1^*$ can be found and the expression $f \sinh^2(\sqrt{K_1'}\, Y^*)$ evaluated as a function of $y^*$. Guesses are made as to the variation of $C_p/C_{p1}$ and $k/k_1$ with $y^*$ and the integral in (5.5) evaluated numerically as a function of $y^*$.

The friction factor $C_f$ can be found from Eq. (4.17) using the mean Reynolds number and the value of $Y_1^*/y_1^*$ from above. Then $F$ is determined from the end value of the integral in (5.5) and the formula:

$$F = \int_0^{y_1^*} \frac{dy^*}{\frac{C_p}{C_{p_1}} f \sinh^2(\sqrt{K_1'}\, Y^*) + \frac{k}{k_1}\frac{1}{\sigma_1}} - 13.89\, \frac{Y_1^*}{y_1^*} \qquad (5.9)$$

and from Eq. (5.7), $C_h$ is found. Making use of the identity:

$$\frac{\rho c_{p_1} u_\tau}{q_0} = \frac{1}{C_h}\sqrt{\frac{C_f}{2}}\,\frac{1}{(T_m - T_w)} \tag{5.10}$$

where the factors on the left hand side are now known, the temperature distribution in the wall layer is determined from (5.5). From this temperature distribution the functions $f$, $C_p/C_{p1}$ and $k/k_1$ are re-determined as functions of $y^*$ and the entire process is repeated until there is no further change in the temperature distribution. Ordinarily, convergence is quite rapid and with a reasonable initial guess as to the variation of $f$, only two numerical integrations of (5.5) are necessary.

An attempt was made to find approximate methods for evaluating the integral in (5.8). The viscosity distribution through the wall layer was represented by a two-parameter family of curves and it was hoped that this would be satisfactory for most liquids. Unfortunately, such a simple representation of the viscosity variation was not sufficiently accurate for the examples studied. The first purpose of the investigation should be a demonstration of the validity of the theory, so that it does not matter if the numerical calculations at this stage are somewhat tedious. At a later time, when the theory is verified and its limitations determined, it will be desirable to find more readily usable approximate formulas.

## VI. COMPARISON OF THEORY OF TRANSPORT FOR VARIABLE PROPERTIES WITH EXPERIMENT

The number of experiments on the influence of variable physical properties on momentum and heat transfer is rather limited and in most experiments the measurements are too inexact for adequate comparison with the theory of the last two sections. In the current standard texts (e.g. Ref. 14) the treatment of heat transfer with variable physical properties is based primarily on the experiments reported in Refs. 15, 16, and 17. The results of these experiments are given in the form of two empirical equations for the friction and heat transfer coefficients, i.e.:

$$C_{f_i}/C_f = \left(\mu_m/\mu_w\right)^{0.14} \tag{6.1}$$

$$C_h = \frac{0.027}{(Re)^{0.2}\,\sigma^{0.67}}\left(\frac{\mu_m}{\mu_w}\right)^{0.14} \tag{6.2}$$

where $C_f$ is the friction coefficient in non-isothermal flow, $C_{fi}$ is the friction coefficient in isothermal flow and the other quantities are defined as in the preceding sections. The viscosity is the only property whose variation is considered and this is assumed to enter only as the ratio of bulk to wall values. The empirical equations above are based on a very limited number of experiments and cannot be expected to have universal validity. The sole serious attempt at a theory for variable viscosity appears to be the semi-empirical work of Boelter and co-workers already described and criticized in Section I.

Within the last two years more accurate experiments on the influence of variable properties have been made at the Jet Propulsion Laboratory by Summerfield and Kreith (Ref. 18). The experiments were restricted to heating fluids at high flux rates but the range of viscosity ratio was extended well beyond that of most previous workers. Three fluids have been investigated, water, aniline and n-butyl alcohol, but the last only is useful for comparison of the theory. The experiments on water gave friction pressure drops thirty percent or so in excess of the values for smooth tubes, thus indicating considerable influence of roughness. Since the theory given here applies only to smooth walls, the comparison of theory with experiment is inconclusive. Further, the Prandtl number for water at the temperatures used in the tests was about 5, a rather low value. The theory is based on the assumption that most of the variation in properties is in the wall layer and a negligible amount in the core. At a Prandtl number of 5, about one-quarter of the temperature difference occurs in the core so the theory applies only approximately. The results of the tests on aniline are also unsatisfactory for comparison with theory because a deposit was formed on the tube surface at the higher heat transfer rates.

The experiments on n-butyl alcohol, as reported in Ref. (18) were made carefully and the accuracy of the measurements is adequate for a comparison with the theory. The bulk temperature in all tests was between 86°F. and 108°F. giving a Prandtl number based on bulk conditions of about 30. The wall temperature was varied from 160°F. to

420°F. so the ratio of bulk viscosity to wall viscosity was varied from 2.25 to 12.7. The bulk Reynolds number was varied from 42,000 to 78,000 in the 58 test runs reported. The heated length of the stainless steel tube was 33 diameters, sufficient that the inlet-length effects should not be serious. Measurements of pressure drop in isothermal flow checked the theory for smooth tubes within two or three percent so it can be assumed that the influence of surface roughness was negligible. The sole difficulty with the final results is that complete knowledge of the dependence of the physical properties of n-butyl alcohol on temperature is not at present available. The conductivity variation, in particular, is not known and although the specific heat and viscosity are better known, the values of these at higher temperatures are extrapolated rather than measured directly.

The test results show an appreciable decrease of friction coefficient as the wall temperature is raised, the coefficient dropping to about half of the isothermal value at a viscosity ratio $\mu_m/\mu_w \cong 10$. The heat transfer coefficient changes very little with viscosity ratio, although there is a slight increase, of the order of 5% to 10% at the maximum wall temperature. The possible experimental errors in the heat transfer measurements are considerably larger than for friction measurements so there is more scatter in the former. For purposes of comparison, eight typical test runs were chosen and the theoretical friction and heat transfer coefficients calculated for the precise conditions of these tests. The analysis was made according to the procedure outlined in the preceding section. No particular advantage

is to be gained from the analysis of more test runs because those chosen cover the range of Reynolds numbers and viscosity ratio of the tests.

The values of the physical properties used in the analysis were taken from the report on the tests (Ref. 18). Variation of the specific heat and viscosity with temperature were taken into account but the conductivity was assumed constant, with $k = 0.095$ Btu/(hr.)(ft.)(°F.). The final results are tabulated below, where the test run numbers are the same as in Ref. 18.

| Run # | Re $\times 10^{-4}$ | $T_m$ (°F.) | $T_w$ (°F.) | $\mu_m/\mu_w$ | $C_{fi}/C$ | | $C_h \times 10^4$ | |
|---|---|---|---|---|---|---|---|---|
| | | | | | Theor. | Exp. | Theor. | Exp. |
| 15 | 7.22 | 94.5 | 163 | 2.35 | 1.152 | 1.15 | 4.70 | 3.66 |
| 17 | 7.19 | 93.8 | 228 | 4.45 | 1.325 | 1.34 | 5.26 | 4.23 |
| 12 | 7.23 | 94 | 320 | 7.23 | 1.687 | 1.67 | 5.56 | 4.23 |
| 13 | 7.59 | 98 | 405 | 12.13 | 1.988 | 1.96 | 5.68 | 4.42 |
| 27 | 4.32 | 97 | 191 | 3.05 | 1.263 | 1.26 | 5.28 | 4.66 |
| 28 | 4.22 | 95 | 245 | 5.01 | 1.450 | 1.47 | 5.56 | 4.60 |
| 33 | 4.28 | 96 | 298 | 7.00 | 1.712 | 1.65 | 5.71 | 4.64 |
| 30 | 4.49 | 100 | 350 | 9.09 | 1.850 | 1.86* | 5.85 | 5.02 |

*(The value reported in Ref. 18 is 1.96, but since this is not consistent with other measurements, the value 1.86 is taken from Run #34, made under almost identical conditions.)

The theoretical and experimental values of $C_{fi}/C_f$ and $C_h$ are plotted in Fig. 4 for easier comparison. The viscosity ratio $\mu_m/\mu_w$ is the parameter having the strongest influence so it is plotted as

the abscissa. The coefficients are actually functions of bulk Reynolds number, bulk Prandtl number and bulk temperature as well, but the range of variation of these in the tests was small and their influence can scarcely be greater than the experimental scatter. The agreement between theoretical and experimental friction coefficients is amazingly good, so good as to appear accidental. Even if the theory were strictly correct it is surprising that the values of the properties and conditions of the experiments as used in the theory do not introduce more error. The minor influence of Reynolds number is apparently predicted quite accurately. The sole major discrepancy is Run #33 and even here the experimental point appears too low because it is out of line with the general trend of the Reynolds number effect. The empirical formula (6.1) does not fit the experimental data except at the lowest viscosity ratios, and of course it does not give any Reynolds number variation.

The theoretical heat transfer coefficients differ appreciably from the measured values, in contrast to the friction coefficients. The analysis predicts a rather rapid increase of heat transfer coefficient with viscosity ratio, tapering off to about 130% of the isothermal value at the highest viscosity ratios. The experiments show a very slight, almost linear increase of heat transfer coefficient with viscosity ratio. The dashed lines were derived from all test runs, not merely the eight given here. These lines represent 13 to 22 experimental points within a maximum scatter of ±6%. Run #15 was

perhaps an unfortunate choice for the analysis because it is one of two points that deviates from the lines by about 12%.

If the theory is reasonably correct, the most likely reason for the overestimation of the heat transfer coefficient is that the variation of conductivity with temperature is neglected in the analysis. It is known that the conductivities of alcohols decrease as the temperature increases. An examination of expression (5.8) for $F$ shows that $F$ will increase if $k$ decreases toward the wall, and as a result $C_h$ will become less. Hence a correct accounting for the variation of $k$ with temperature will certainly tend to decrease the discrepancy between theory and experiment. The variation of $k$ will modify the temperature distribution close to the wall, giving a different viscosity variation and hence change the friction coefficient. This effect will be secondary, however, compared with the change of heat transfer coefficient, as can be seen from (5.5) or (5.8). The conductivity variation appears in the second term of the denominator of the integrand and this term is dominating at the wall or very close to the wall where $k$ will be smallest. The first term, which alone involves the viscosity variation, becomes important a certain distance away from the wall and will not be very strongly influenced by the change of temperature distribution closer to the wall. Hence agreement of the theoretical and experimental heat transfer coefficients does not necessitate disagreement of the friction coefficients.

Variation of the conductivity was not taken into account in the analysis because very little information concerning the dependence on

temperature is available. The only measurements reported appear to be those of Bridgman who found $k = 0.097$ Btu/(hr.)(ft.)(°F.) at 86°F. and $k = 0.094$ at 167°F. for n-butyl alcohol. Conductivities at higher temperatures are lacking, even for similar liquids. In order to bring theory and experiment into agreement, the value of the conductivity should decrease with temperature at a decreasing rate so that its value at 400°F. is 60% to 70% of the value at 90°F.. This requirement does not seem consistent with the results of Bridgman's measurements, although the latter may not be completely reliable.

The conclusions regarding the theory which can be derived from the comparison above are not as definite as desired. The mechanism of turbulent transport of momentum as postulated cannot be far wrong, otherwise the friction coefficients would not agree so well. The mechanism of energy transport assumed in the analysis may be quantitatively correct but this cannot be proved or disproved until the conductivity variation with temperature is known. No other experiments of sufficient accuracy for comparison with the theory are known. In this connection it is interesting to note that the empirical formula (6.2) for the heat transfer coefficient, derived from earlier experiments, underestimates the coefficients reported in Ref. 18 by about 20% and requires a change of the exponent of the viscosity ratio from 0.14 to 0.10 to give satisfactory agreement. Even if the turbulent transport mechanism postulated here is not quite correct, it is obvious from the analytical forms that no simple equations such as (6.1) and (6.2) can

possibly have universal validity. Simplification of the analysis used here can undoubtedly be gained by approximations, but until the limitations of the theory are better known there seems to be little point in introducing them at this stage.

## REFERENCES


1. Reynolds, O.- Collected Papers I., pp. 81-85.
2. Taylor, G. I. - A.R.C. Reports and Memoranda No. 272, 1919.
3. Prandtl, L. - Physik. Zeitsch. 29, 1928, pp. 487-489.
4. von Kármán, Th. - Proc. 4th Int. Cong. for App. Mech. 1934, pp. 54-91.
5. von Kármán, Th. - The Analogy between Fluid Friction and Heat Transfer, Trans. A.S.M.E. 61, 1939, pp. 705-710.
6. Goldstein, S. (Editor) - Modern Developments in Fluid Mechanics, Vol. II., Oxford, 1938.
7. Reichardt, H. - Die Wärmeübertragung un turbulenten Reibungsschichten, ZAAM, 20, 1940, pp. 297-328.
8. Boelter, L. M. K., Martinelli, R. C. and Jonassen, F. - Analogy between Heat and Momentum Transfer, Trans. A.S.M.E. 63, 1941, pp. 447-455.
9. Martinelli, R. C. - Heat Transfer to Molten Metals, Trans. A.S.M.E. 63, 1941, pp. 447-455.
10. von Kármán, Th. - Proc. 3rd Int. Cong. for App. Mech., Stockholm, 1930, pp. 85-92.
11. Laufer, J. - Some Recent Measurements in a Two-Dimensional Turbulent Channel, Jour. Aero. Sc. 17, 1950, pp. 277-287.
12. Corrsin, S. - Investigation of Flow in an Axially Symmetrical Heated Jet of Air, NACA Wartime Report W-94.

13. Sage, B. H. - unpublished communication.

14. McAdams, W. H. - Heat Transmission, 2nd ed. McGraw-Hill, 1942.

15. Morris, F. H. and Whitman, W. G. - Heat Transfer for Oil and Water in Pipes, Ind. and Eng. Chem. 20, 1928, p. 234.

16. Sieder, E. N. and Tate, G. E. - Heat Transfer and Pressure Drops of Liquids in Tubes, Ind. and Eng. Chem. 28, 1936, pp. 1429-1436.

17. Smith, J. F. D. - Heat Transfer and Pressure Drop Data for an Oil in a Copper Tube, Trans. Am. Inst. Chem. Eng. 31, 1934, pp. 83-111.

18. Kreith, F. and Summerfield M. - Investigation of Heat Transfer at High Heat Flux: Experimental Study of Heat Transfer and Friction Drop with n-Butyl Alchohol in an Electrically Heated Tube, Progress Report No. 4-95, Jet Propulsion Laboratory, May 17, 1949, (to be published shortly in the Trans. A.S.M.E.).

## APPENDIX A.

The momentum equation for flow with axial symmetry in a pipe is, for an incompressible fluid:

$$r\frac{\partial u}{\partial t} + \frac{\partial}{\partial r}(ruv) + \frac{\partial}{\partial x}(ru^2) = -\frac{1}{\rho}\frac{\partial p}{\partial x}r + \frac{1}{\rho}\frac{\partial}{\partial r}\left(\mu r\frac{\partial u}{\partial r}\right) + \frac{1}{\rho}\frac{\partial}{\partial x}\left(\mu r\frac{\partial u}{\partial x}\right) \qquad (1)$$

where $u$ and $v$ are components of velocity in the radial and axial directions. For fully-established turbulent flow, $u = \bar{u} + u'$, $v = v'$, $p = \bar{p} + p'$, where the barred quantities are time averages, assumed functions of position only, and the primed quantities represent the turbulent fluctuations. Substituting these into Eq. (1), averaging with respect to time and dropping derivatives with respect to x, except for p,

$$\frac{d}{dr}\left(r\overline{u'v'}\right) = -\frac{1}{\rho}\frac{dp}{dx}r + \frac{1}{\rho}\frac{d}{dr}\left(\mu r\frac{du}{dr}\right) \qquad (2)$$

The form of this result implies that $p$ is a function of $x$ alone and the other terms are functions of $r$ alone, in conformity with the assumption of fully-established turbulent flow.

The shear stress at the wall of the pipe is $\tau_o = -\frac{1}{2R}\frac{dp}{dx}$ where R is the pipe radius. Substituting into Eq. (2) and integrating with respect to:

$$r\overline{u'v'} = \frac{1}{\rho}\frac{\tau_o}{R}r^2 + \frac{1}{\rho}\mu r\frac{du}{dr}$$

The constant of integration is zero, since $\tau_o = \mu\frac{du}{dr}$ at the wall.

Dividing through by $r$ and rearranging:

$$-\tau_0 \frac{r}{R} = -\rho\overline{u'v'} + \mu \frac{du}{dr}$$

In terms of distance $y$ from the wall, putting $r = R - y$ and changing the sign of $v'$, this equation becomes:

$$\tau_0 (1 - y/R) = -\rho\overline{u'v'} + \mu \frac{du}{dy} \tag{3}$$

For $y << R$ the left-hand side of this equation becomes simply $\tau_0$. Strictly, the factor $1-y/R$ should be left in the equation to give correct results near the center of the pipe; for instance, to make $du/dy = 0$ at $y = R$. At high Reynolds numbers, however, the resulting velocity distribution differs from the approximate form by a negligible amount. At lower Reynolds numbers, for instance, 2000 to 10,000, the form of $\overline{u'v'}$ is not known precisely anyway and the addition of the factor $(1-y/R)$ may not improve the result appreciably.

The energy equation applicable to flow in a pipe is similar in form to the momentum equation. If $h$ is the specific enthalpy of the fluid

$$r\frac{\partial h}{\partial t} + \frac{\partial}{\partial r}(rhv) + \frac{\partial}{\partial x}(rhu) = \frac{1}{\rho}\frac{\partial}{\partial r}\left(kr\frac{\partial T}{\partial r}\right) + \frac{1}{\rho}\frac{\partial}{\partial x}\left(kr\frac{\partial T}{\partial x}\right) \tag{4}$$

where the pressure and dissipation terms have been neglected. Putting $h = \bar{h} + h'$, $u = \bar{u} + u'$ and $v = v'$, into Eq. (4), and averaging with respect to time, for steady flow:

$$\frac{\partial}{\partial r}\left(r\overline{h'v'}\right) + \frac{\partial}{\partial x}\left(r\bar{h}\bar{u} + r\overline{h'v'}\right) = \frac{1}{\rho}\frac{\partial}{\partial r}\left(kr\frac{\partial \bar{T}}{\partial r}\right) + \frac{1}{\rho}\frac{\partial}{\partial x}\left(kr\frac{\partial \bar{T}}{\partial x}\right) \tag{5}$$

One cannot assume that $\bar{h}$ is independent of $x$, because then no heat can flow into the system. The only "fully-developed" temperature profile is one with constant temperature everywhere. If the temperature gradient along the pipe is small compared with the radial gradient, one can neglect the terms $\frac{\partial}{\partial x}\left(\overline{h'u'}\right)$ and $\frac{1}{\rho}\frac{\partial}{\partial x}\left(k\frac{\partial \bar{T}}{\partial x}\right)$ in comparison with the others. The term $\frac{\partial}{\partial x}\left(r\bar{h}\bar{u}\right)$ is retained to allow for heat flux at the wall.

With the assumptions above, the energy equation becomes:

$$\frac{\partial}{\partial x}\left(r h u\right) = \frac{\partial}{\partial r}\left(-r\overline{h'v'} + \frac{k}{\rho} r \frac{\partial T}{\partial r}\right) \tag{6}$$

where the bars over h, u and T are dropped. The velocity distribution u is a known function of $r$ alone. Eq. (6) is a partial differential equation and is, of course, difficult to solve except for very special boundary conditions. It is usual practice to assume that the heat flux per unit area normal to the radius is of the form $q = q_0 r/R$ where $q_0$ is the value at the wall. This is strictly true of $\partial h/\partial x$ is constant over the cross-section. Then from a heat balance:

$$\int_0^r r \frac{\partial h}{\partial x} u \, dr = -\frac{q}{\rho} r = -\frac{q_0}{\rho}\frac{r^2}{R} \tag{7}$$

With this result, integration of Eq. (6) yields:

$$-q_0 \frac{r}{R} = -\rho \overline{h'v'} + k\frac{dT}{dr}$$

and substituting $r = R - y$ with a change in the sign of $v'$ :

$$q_0\left(1 - y/R\right) = -\rho\overline{h'v'} + k\frac{dT}{dr} \tag{8}$$

This equation is now identical in form with Eq. (3), but is more restricted in application. It should be satisfactory after a heated length of pipe of twenty or so diameters, provided that the conductivity is not very large.

It has been assumed in all of the analysis of this paper that the influence of the viscosity fluctuations is negligible. This assumption appears valid, although no positive proof can be given. With viscosity a function of temperature only, the viscosity fluctuations can be approximated by:

$$\mu' = \frac{d\mu}{dT} T'$$

since $T'$ is ordinarily small. For a flat wall, the term involving viscosity is:

$$\frac{\partial}{\partial y}\left[\mu\left(\frac{\partial u}{\partial x} + \frac{\partial v}{\partial y}\right)\right]$$

Putting $u = \bar{u} + u'$ , $v = v'$ , $\mu = \bar{\mu} + \frac{d\mu}{dT} T'$ and averaging, this term becomes:

$$\frac{\partial}{\partial y}\left(\bar{\mu}\,\frac{\partial \bar{u}}{\partial y}\right) + \frac{\partial}{\partial y}\left[\frac{d\bar{\mu}}{dT}\,\overline{T'\left(\frac{\partial u'}{\partial y} + \frac{\partial v'}{\partial x}\right)}\right]$$

Hence, one should add to the right-hand side of Eq. (3) the term:

$$\frac{d\mu}{dT}\,\overline{T'\left(\frac{\partial u'}{\partial y} + \frac{\partial v'}{\partial x}\right)}$$

Certainly for higher Prandtl numbers $d\mu/dT$ is large only very close to the wall; in this region, however, the turbulent fluctuations are small.

Further from the wall, where the fluctuations are larger, $d\mu/dT$ is small. Hence, it seems reasonable to assume that the entire term is small everywhere.

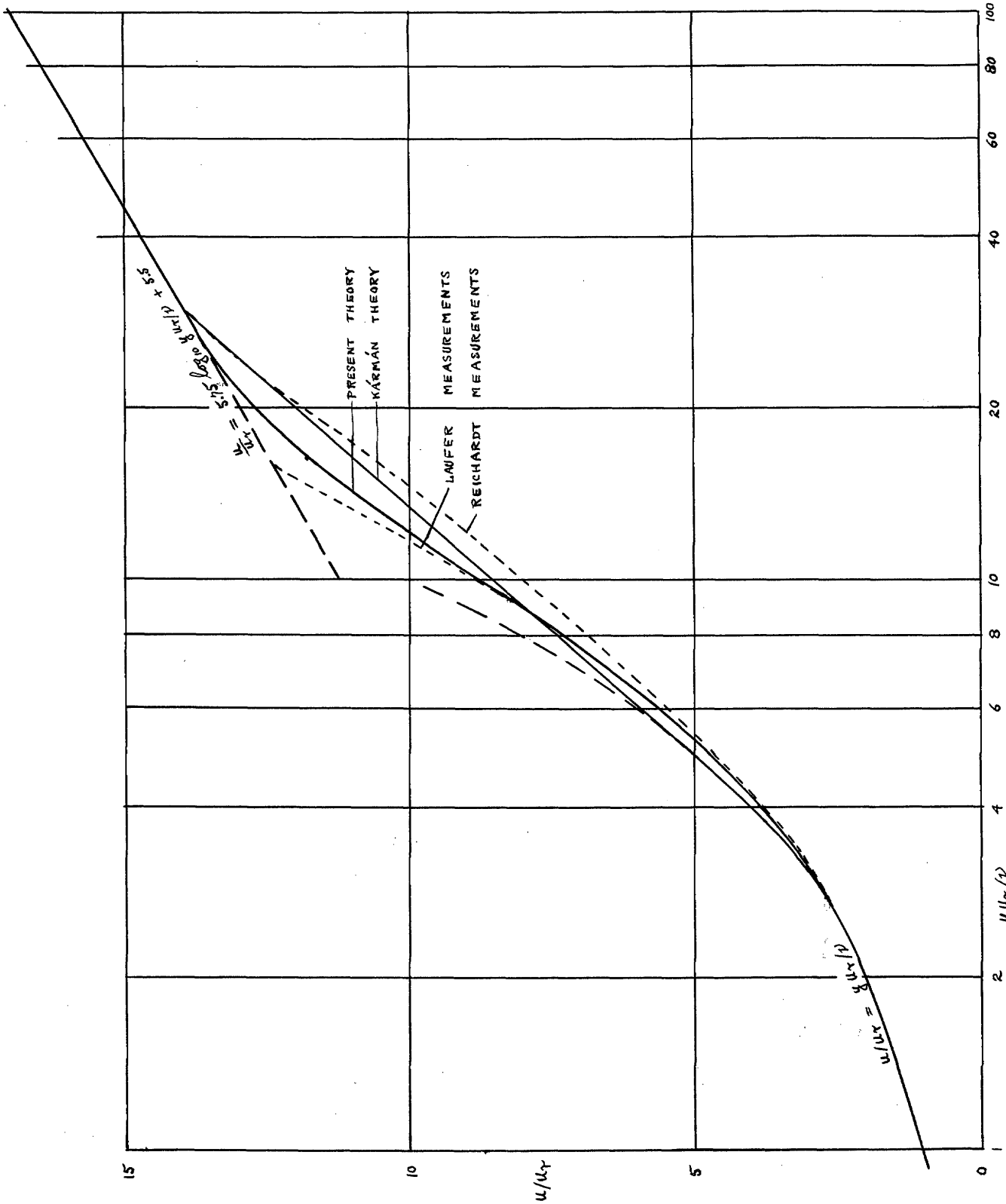


FIG. 1 COMPARISON OF VELOCITY PROFILES

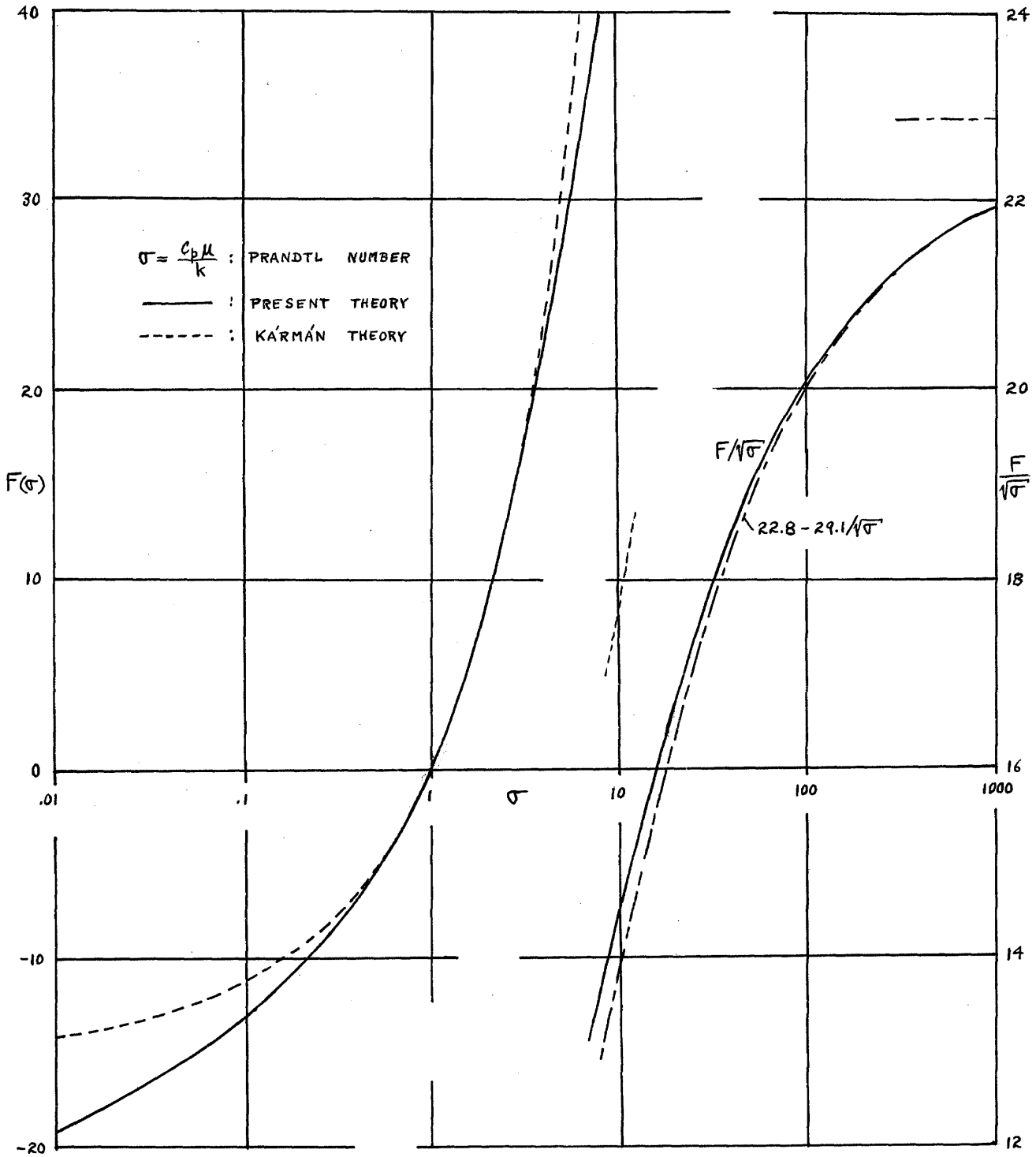


FIG. 2 THE FUNCTION $F(\sigma)$ IN $\frac{1}{C_h} = \frac{2}{C_f} + F(\sigma)\sqrt{\frac{2}{C_f}}$

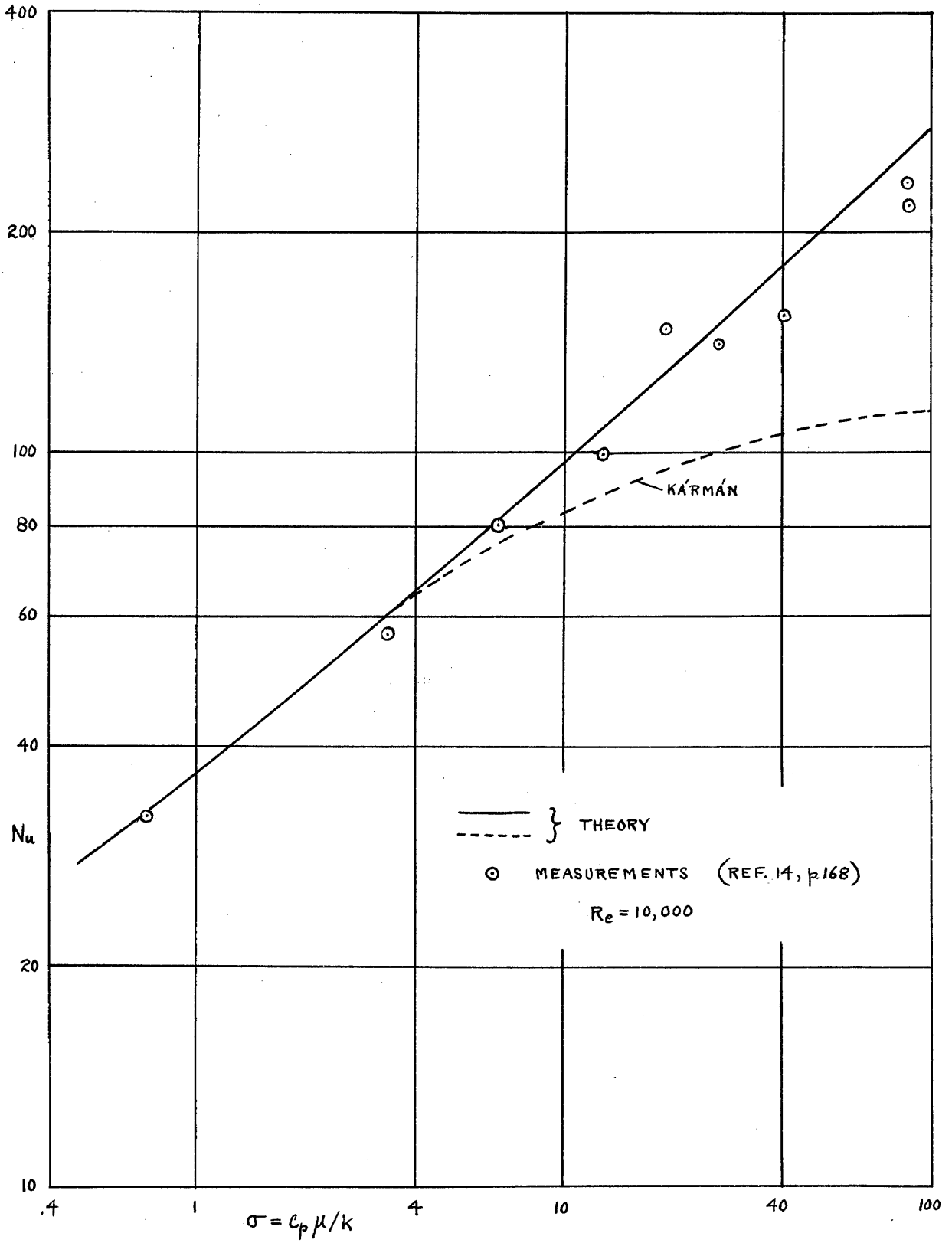


FIG. 3 COMPARISON OF THEORETICAL HEAT TRANSFER COEFFICIENTS WITH MEASUREMENTS AT VARIOUS σ

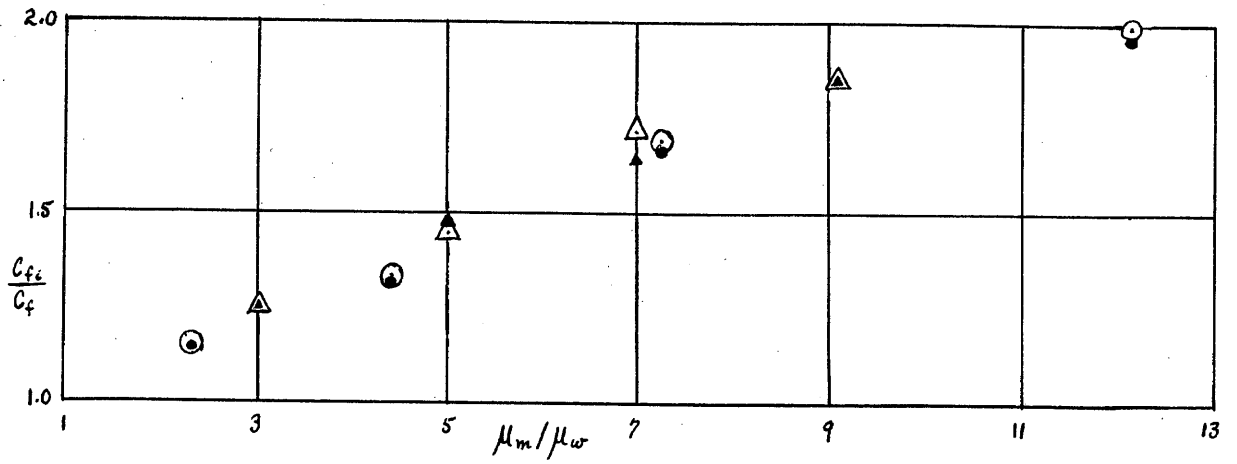


FIG. 4(a) COMPARISON OF THEORETICAL FRICTION COEFFICIENTS WITH MEASUREMENTS OF SUMMERFIELD AND KRIETH

$\mu_m$ : BULK VISCOSITY

$\mu_w$ : WALL VISCOSITY

$C_{fi}$ : ISOTHERMAL FRICTION COEFFICIENT AT SAME BULK REYNOLDS NUMBER

⊙ THEORY
• MEASUREMENT
} $Re \cong 7.4 \times 10^4$

△ THEORY
▲ MEASUREMENT
} $Re \cong 4.4 \times 10^4$

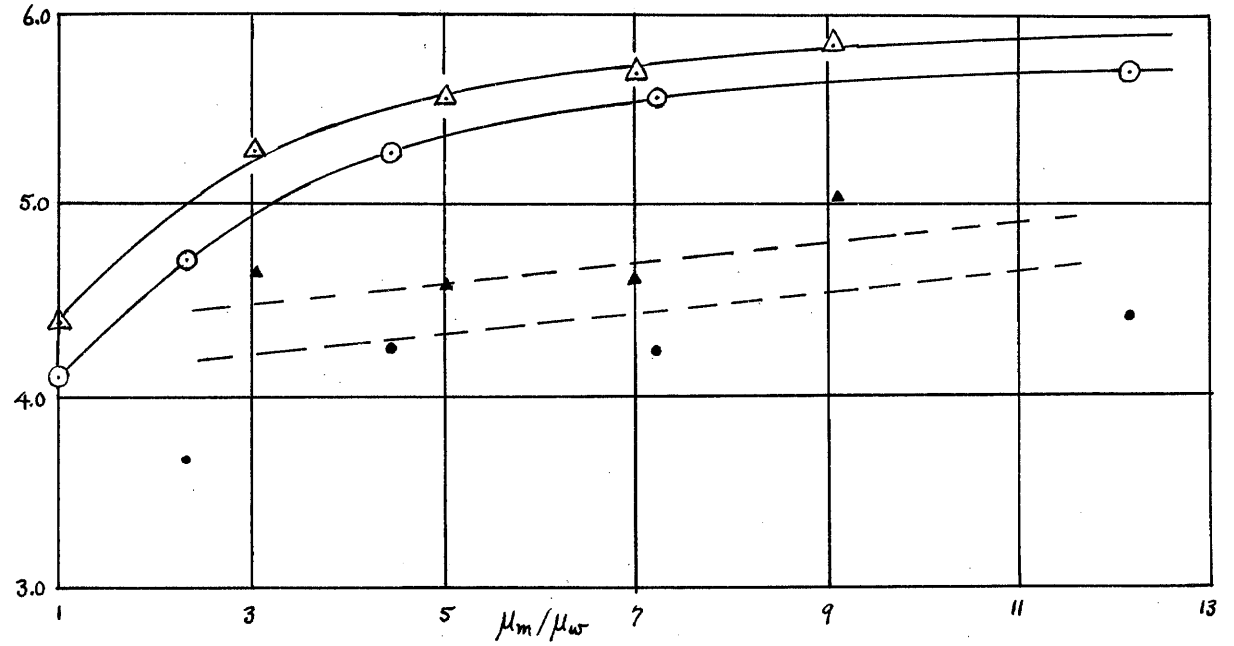


FIG. 4(b) COMPARISON OF THEORETICAL HEAT TRANSFER COEFFICIENTS WITH MEASUREMENTS OF SUMMERFIELD AND KRIETH